

AD-A042 341

NAVAL POSTGRADUATE SCHOOL MONTEREY CALIF

F/6 20/5

A HYDROGEN FLUORIDE/DEUTERIUM FLUORIDE LASER AT THE NAVAL POSTG--ETC(U)

JUN 77 W T FUNK, R F SONTHEIMER

UNCLASSIFIED

NL

1 OF 1  
AD  
A042341



END

DATE  
FILMED  
8-77

AD A 042341

2  
B. S.

# NAVAL POSTGRADUATE SCHOOL

Monterey, California



## THESIS

A HYDROGEN FLUORIDE/DEUTERIUM FLUORIDE  
LASER AT THE NAVAL POSTGRADUATE SCHOOL

by

William Ted Funk

and

Richard Francis Sontheimer

June 1977

Thesis Advisor:

A. W. Cooper

Approved for public release; distribution unlimited.

AD No. \_\_\_\_\_  
DDC FILE COPY



UNCLASSIFIED

SECURITY CLASSIFICATION OF THIS PAGE (When Data Entered)

REPORT DOCUMENTATION PAGE		READ INSTRUCTIONS BEFORE COMPLETING FORM
1. REPORT NUMBER	2. GOVT ACCESSION NO.	3. RECIPIENT'S CATALOG NUMBER (7)
4. TITLE (and Subtitle) A Hydrogen Fluoride/Deuterium Fluoride Laser at the Naval Postgraduate School.		5. TYPE OF REPORT & PERIOD COVERED Master's Thesis June 1977
7. AUTHOR(s) William Ted Funk Bernard Francis Sontheimer		6. PERFORMING ORG. REPORT NUMBER
8. PERFORMING ORGANIZATION NAME AND ADDRESS Naval Postgraduate School Monterey, CA 93940		9. CONTRACT OR GRANT NUMBER(s)
11. CONTROLLING OFFICE NAME AND ADDRESS Naval Postgraduate School Monterey, CA 93940		10. PROGRAM ELEMENT, PROJECT, TASK AREA & WORK UNIT NUMBERS
14. MONITORING AGENCY NAME & ADDRESS (if different from Controlling Office) Naval Postgraduate School Monterey, CA 93940		12. REPORT DATE June 1977
		13. NUMBER OF PAGES 92
		15. SECURITY CLASS. (of this report) UNCLASSIFIED
		15a. DECLASSIFICATION/DOWNGRADING SCHEDULE
16. DISTRIBUTION STATEMENT (of this Report) Approved for public release; distribution unlimited (12) 91 P.		
17. DISTRIBUTION STATEMENT (of the abstract entered in Block 20, if different from Report)		
18. SUPPLEMENTARY NOTES		
19. KEY WORDS (Continue on reverse side if necessary and identify by block number) Hydrogen Fluoride Deuterium Fluoride Infrared Chemical Laser Atmospheric Propagation		
20. ABSTRACT (Continue on reverse side if necessary and identify by block number) A small scale hydrogen fluoride (HF) or deuterium fluoride (DF) laser was constructed for the Atmospheric Optical Propagation Program at the Naval Postgraduate School. The laser, with almost forty individually selectable wavelengths between 2.5 and 4.1 micrometers, will prove to be a valuable instrument for the continued studies of laser propagation.  In the HF mode, a multiline power out of seven watts was achieved with		

DD FORM 1 JAN 73 1473

EDITION OF 1 NOV 68 IS OBSOLETE  
S/N 0102-014-6601

UNCLASSIFIED

SECURITY CLASSIFICATION OF THIS PAGE (When Data Entered)

251 450 1

UNCLASSIFIED

SECURITY CLASSIFICATION OF THIS PAGE (When Data Entered)

a confocal cavity arrangement. In the single-line HF mode, fifteen separate wavelengths were distinguished. Three watts of multiline power was achieved in the DF mode while eighteen separate single-line wavelengths were obtained including 160 milliwatts at 3.8007 micrometers, the  $P_2(8)$  transition. This wavelength is of particular interest to the Navy because of its excellent propagation characteristics in the marine boundary layer.

ADDITIONAL	
NTIS	NTIS SOURCE <input checked="" type="checkbox"/>
DOC	Ref Section <input type="checkbox"/>
UNANNOUNCED	<input type="checkbox"/>
JUSTIFICATION	
BY	
DISTRIBUTION/AVAILABILITY CODES	
Dist.	AVAIL. 201/01 SPECIAL
A	



Approved for public release; distribution unlimited

A Hydrogen Fluoride/Deuterium Fluoride Laser  
at the Naval Postgraduate School

by

William Ted Funk  
Lieutenant, United States Navy  
B.S., University of Kansas, 1971

Richard Francis Sontheimer  
Lieutenant, United States Navy  
B.S., University of New Mexico, 1971

Submitted in partial fulfillment of the  
requirements for the degree of

MASTER OF SCIENCE IN PHYSICS

from the

NAVAL POSTGRADUATE SCHOOL  
June 1977

Authors:

*William T. Funk*  
-----  
*Richard Sontheimer*  
-----

Approved by:

*aw cooper*  
----- Thesis Advisor  
*William M. Tolles*  
----- Second Reader  
*H. E. Wacker*  
----- Chairman, Department of Physics and Chemistry  
*Robert A. Jernigan*  
----- Dean of Science and Engineering

# ABSTRACT

A small scale hydrogen fluoride (HF) or deuterium fluoride (DF) laser was constructed for the Atmospheric Optical Propagation Program at the Naval Postgraduate School. The laser, with almost forty individually selectable wavelengths between 2.5 and 4.1 micrometers, will prove to be a valuable instrument for the continued studies of laser propagation.

In the HF mode, a multiline power out of seven watts was achieved with a confocal cavity arrangement. In the single-line HF mode, fifteen separate wavelengths were distinguished. Three watts of multiline power was achieved in the DF mode while eighteen separate single-line wavelengths were obtained including 160 milliwatts at 3.6007 micrometers, the  $P_2(8)$  transition. This wavelength is of particular interest to the Navy because of its excellent propagation characteristics in the marine boundary layer.

## TABLE OF CONTENTS

I.	INTRODUCTION.....	10
A.	BACKGROUND.....	10
B.	ATMOSPHERIC PROPAGATION.....	11
II.	THEORY OF OPERATION.....	16
A.	ENERGY LEVELS OF A DIATOMIC MOLECULE.....	16
B.	HF/DF CHEMISTRY.....	22
1.	The Chemical Reaction.....	22
2.	A Qualitative Description of Fluorine and Hydrogen Fluoride.....	25
C.	THE OPTICAL RESONATOR.....	26
1.	Multi-line Operation.....	26
2.	Single-line Operation.....	27
III.	THE HF/DF LASER AT THE NAVAL POSTGRADUATE SCHOOL.	30
A.	EQUIPMENT LOCATION.....	30
B.	EQUIPMENT DESCRIPTION.....	31
1.	The Laser Bench.....	31
2.	Laser Support Systems.....	36
a.	Gas Supply System.....	36
b.	Water Cooling System.....	36
c.	DC Power Supply.....	37
d.	Vacuum System.....	38
e.	Scrubber System.....	39
f.	Detector System.....	40
C.	EQUIPMENT OPERATION.....	41
1.	Multiline Alignment Procedure.....	41
2.	Single-Line Alignment and Operation.....	42
3.	Laser Start-up and Shut-down Procedures..	43
D.	LASER PERFORMANCE.....	45
1.	HF Performance.....	45
a.	Multiline Performance.....	45

b. Single-line Performance.....	47
2. DF Performance.....	49
a. Multiline Performance.....	49
b. Single-line Performance.....	50
3. Portable Performance Study.....	52
Appendix A: LASER SUPPLIES.....	54
Appendix B: START UP PROCEDURES.....	55
Appendix C: SHUT DOWN PROCEDURES.....	56
Appendix D: FIGURES.....	57
LIST OF REFERENCES.....	89
INITIAL DISTRIBUTION LIST.....	91
LIST OF TABLES.....	7
LIST OF FIGURES.....	8



## LIST OF TABLES

I. Molecular Transitions of HF and DF.....	22
II. Single-line Selection Settings.....	44

## LIST OF FIGURES

1. Water Vapor Transmission (2.4-5.2 micrometers) .....	57
2. Atmospheric Transmission (1.7-3.0 micrometers) .....	58
3. Atmospheric Transmission (3.0-4.2 micrometers) .....	59
4. Power out versus Transmission Coefficient (HP) .....	60
5. The Diffraction Grating .....	61
6. Tunable Single-line Diagram .....	62
7. Tunable Single-line Adapter .....	63
8. Tunable Single-line Installation .....	64
9. Electrical Supply Schematic .....	65
10. Laser Room-External View .....	66
11. Laser Bench-Top View .....	67
12. Laser Bench-Front View .....	68
13. Laser Bench--Single-line Installation .....	69
14. The Mixing Chamber Diagram .....	70
15. The Mixing Chamber Opened .....	71
16. The Optical Resonator .....	72
17. The Geometry of the Optical Resonator .....	73
18. The DC Power Supply .....	74
19. Vacuum System Schematic .....	75
20. Vacuum Pump .....	76

21.	Scrubber System Diagram.....	77
22.	Scrubber System.....	78
23.	Laser Control Panel Diagram.....	79
24.	The Hydrogen Fluoride Flame.....	80
25.	Laser Alignment Diagram.....	81
26.	Beam Radius--DF Single-line Operation.....	82
27.	Output Power-H <sub>2</sub> or D <sub>2</sub> Flow Rate Variations.....	83
28.	Output Power-SF <sub>6</sub> Flow Rate Variations.....	84
29.	Output Power-O <sub>2</sub> Flow Rate Variations.....	85
30.	Output Power-He Flow Rate Variations.....	86
31.	HF Wavelengths.....	87
32.	DF Wavelengths.....	88

## I. INTRODUCTION

### A. BACKGROUND

The laser, or optical maser, was proposed as an aside from the then current studies of microwave amplifying devices called masers by Arthur L. Schawlow and Charles H. Townes in a published paper in 1958. Theodore H. Maiman then built the first laser, a pulsed ruby laser, in 1960. In 1961 Ali Javan successfully achieved continuous wave lasing action with a helium-neon infra-red device. Around 1967, several noted scientists active in the laser field began investigating possible gas dynamic chemical lasers. Their work culminated in 1969 when J. R. Airey et al. of AVCO Everett Research Laboratories and D. J. Spencer et al. of Aerospace Corporation simultaneously observed lasing action from a supersonic diffusion flame utilizing HF/DF as a lasing medium.

The use of fluorine as a reactant in a chemical laser follows naturally from the fact that the conversion of chemical energy into coherent radiation of optimum power can be obtained with the minimum amount of non-chemical energy added. The hydrogen-fluoride heat of reaction is 14.6 KJ/gm [3] of fluorine of which 60% appears exothermally in vibrational excitation of HF/DF molecules and the remainder is lost as rotational and translational energy.

In 1970, J.J. Hinchey reported successful laser action from a transverse flow, subsonic, electrical discharge



device using  $SF_6$  as a source of fluorine atoms. Sulfur hexafluoride being non-toxic and non-corrosive was chosen as an alternative to  $F_2$  or  $SF_4$ , the latter two being dangerous and difficult to handle. One drawback of  $SF_6$  is that it requires a high power electric arc to dissociate it to obtain free fluorine atoms. Because of the high electrical power input, subsonic flow, and single-pass gain through the lasing medium, the Hinch design is inherently a low power, highly stable, low cost laboratory device capable of about 15 watts multi-line and 4 watts single-line operation.

As an integral part of the ongoing Atmospheric Optical Propagation experiment at the Naval Postgraduate School, Aerospace Corporation was contracted to construct a HF/DF laser head of the Hinch design. This thesis describes the assembly of this laser and ancillary equipment into an operational portable laboratory laser in the 2.5 to 4.1 micrometer region.

## B. ATMOSPHERIC PROPAGATION

Optical transmission of energy is generally expressed by the fractional transmission or transmittance

$$T = \exp(-\sigma Z), \quad (1-1)$$

where  $\sigma$  is the attenuation coefficient or extinction coefficient and  $Z$  is the length of the transmission path. The attenuation coefficient is the result of two processes-scattering and absorption. The scattering portion is further broken down to functions of particle size, distribution and number density, and particle composition. Although these quantities vary both periodically and

randomly with time and position, measurements of the statistical determinators can allow an approximate prediction of the attenuation using standard models for the atmospheric composition. These statistical measures can be obtained from analysis of the laser beam propagation parameters.

The measurement of scintillation, modulation transfer function (MTF), beam or image wander and spread, scattering, and absorption over a given distance with known meteorological data will allow approximate prediction of the effects of these parameters on laser beam propagation through similar conditions.

Beam spread, wander, and scintillation are direct results of local perturbations in the refractive index caused by turbulence or heat gradients. The locally perturbed medium may be viewed as a mixture of various sized glass marbles. Considering a unit volume of these marbles, the total irradiance received at any point is made up of many components of energy which have traveled over different ray paths. With the above described atmospheric model varying with time, scintillation and beam spread will occur. If the turbules are large enough, beam wander occurs. Scattering occurs when the beam is deflected off of particles in suspension in the air. Particles such as dust, water vapor, haze and other combustion products are the main concern when considering scattering.

At the infrared end of the light spectrum and the one with which this thesis will be concerned, the phenomenon of absorption by atmospheric constituents is the overriding factor in the selection of usable wavelengths. Beer's law states that the spectral transmittance is [1]:

$$T(\nu) = I/I_0 = \exp(-K_\nu U) \quad (1-2)$$

where  $K_\nu$  is the absorption coefficient at the wave number  $\nu$  and  $U$  is the mass of absorbing gas per unit area. The fractional radiant absorptance,  $A$ , over a finite wave number interval,  $\nu_1$  to  $\nu_2$ , is defined as

$$A = \int_{\nu_1}^{\nu_2} [1 - \exp(-K_\nu U)] d\nu \quad (1-3)$$

The absorption coefficient for the collision dominated line shape appropriate for most atmospheric problems is the Lorentz form

$$K = (S/\pi)\alpha / [(\nu - \nu_0)^2 + \alpha^2] \quad (1-4)$$

where  $S$  is the total line intensity and  $\alpha$  is the half-width at the half-maximum (HWHM) of the spectral line whose center is located at the wave number  $\nu_0$ . According to kinetic theory, the half-width at half-maximum depends both on total pressure,  $p$ , and absolute temperature,  $T$ , giving

$$\alpha = \alpha_0 (p/p_0) (T_0/T)^{1/2} \quad (1-5)$$

where  $p_0$  and  $T_0$  are defined as the pressure and temperature at a predefined standard condition. Since the partial pressures of the absorbing species are normally small,  $\alpha$  varies with the total atmospheric pressure while  $U$  is determined only by the partial pressure of the absorber. For the ease of manipulation, new variables are defined as

$$x = SU/2\pi\alpha$$

and

$$\nu' = (\nu - \nu_0) / \alpha.$$

Equation (1-3) now becomes

$$A = \alpha \int_{-\infty}^{\infty} [1 - \exp(-2x / (1 + \nu'^2))] d\nu' \quad (1-6)$$

Assuming there is no absorption outside of the interval  $\nu_1$  to  $\nu_2$ , the limits of integration were extended to infinity.

There are two limiting results for absorptance which can be obtained from (1-6); the weak-line and strong-line approximations. When the path length is small or the total pressure high the exponential in (1-6) is small for all values of  $\nu$ , and the exponential may be approximated by the first two terms of its series expansion. The absorptance can then be given as [1]:

$$A = 2\pi\alpha x = SU; x \leq 0.2 \quad (1-7)$$

When either the path length is large or the total pressure is low, the absorption may be complete over a wave number region of several half-widths. It is in this region that the strong-line approximation is valid. It is given by [1]:

$$A = 2(S\alpha U)^{1/2}; x \geq 1.63. \quad (1-8)$$

In the weak-line region, (1-7), absorptance increases linearly as path length and line intensities increase. In the strong-line approximation region, (1-8), known as the square root region, the absorptance varies as the square root of the path length, pressure, and line intensity. Both (1-7) and (1-8) when used within their limiting region are accurate to within 10% [1].

The above results can now be utilized to obtain theoretical transmittances for various wavelengths and

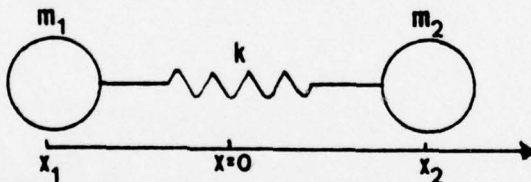


concentrations normally found in the atmosphere. The spectral transmittance can be obtained by the summation of all the absorption coefficients for all expected transitions of the species present. The total transmittance,  $T$ , can then be determined by the integration of the summation over the bandwidth. For laser beam transmission the bandwidth must be considered zero, or the resolution infinite. For operation in the marine boundary layer the high partial pressure of water in the atmosphere causes severe attenuation for most laser sources. Fig 1 [2] indicates the low resolution calculated transmission versus wavelength values in the HF/DF laser region for various water vapor concentrations. Figs 2 and 3 [2] show measured atmospheric transmission through a marine boundary layer at a distance of 300 meters for wavelengths 1.7 to 4.2 micrometers. Using these results and the fact that most of the vibrationally-excited DF transitions occur between 3.5 and 3.9 micrometers the DF laser is the most desirable laser to operate at sea level in the infrared region. In particular the  $P_2(8)$  line at 3.8007 micrometers shows about 97% transmission over 10Km at sea level.

## II. THEORY OF OPERATION

### A. ENERGY LEVELS OF A DIATOMIC MOLECULE [4]

To properly understand how the HF/DF diatomic molecule emits photons in the 2.5 to 4.1 micrometer range, a quantum mechanical model of the energy levels of the molecules must be derived and evaluated. To begin with, consider a model of two nuclei held together by an internuclear bonding strength that will be approximated by a harmonic potential well. This model will have the ability to simulate the vibration and rotation characteristics of the molecule, but each characteristic will be examined separately and then combined into a complete model. The vibrational model is shown below



where  $m_1$ =mass of atom 1,  $m_2$ =mass of atom 2, and  $k$ =harmonic potential well constant approximating the interatomic bonding force of the molecule. The potential energy  $V$  and kinetic energy  $T$  can be described as:

$$V = 1/2k(x_2 - x_1)^2 \quad (2-1)$$

$$T = 1/2(m_1 \dot{x}_1^2 + m_2 \dot{x}_2^2) \quad (2-2)$$

where

$$\dot{x} = dx/dt$$

Now for ease of manipulation, transform V and T to a center of mass coordinate  $q_2$  and difference coordinate  $q_1$  defined as:

$$q_2 = (m_1 x_1 + m_2 x_2) / (m_1 + m_2)$$

$$q_1 = x_2 - x_1$$

$$M = m_1 + m_2$$

$$m_r = (m_1 m_2) / (m_1 + m_2)$$

where M is the total mass of the diatomic molecule and  $m_r$  is the reduced mass. With the above definitions, the kinetic energy equation becomes:

$$T = 1/2 (M \dot{q}_2^2 + m_r \dot{q}_1^2) \quad (2-3)$$

and the potential energy equation becomes:

$$V = 1/2 k q_1^2 \quad (2-4)$$

where

$$\dot{q} = dq/dt$$

The classical hamiltonian ( $H = T + V$ ) is given by:

$$H = T + V = 1/2 M \dot{q}_2^2 + 1/2 m_r \dot{q}_1^2 + 1/2 k q_1^2 \quad (2-5)$$

The quantum mechanical hamiltonian is now obtained by substituting the suitable derivative operators giving

$$\mathcal{H} = (-\hbar^2/2) [ 1/M (\partial^2/\partial q_2^2) + 1/m_r (\partial^2/\partial q_1^2) ] + 1/2 k q_1^2 \quad (2-6)$$

The energy eigenvalues are now found by using the Schrodinger wave equation

$$\mathcal{H}\psi = E\psi$$

The vibrational and translational coordinates are separable. After separating out the translational portion, the vibrational portion becomes

$$E_v \psi(q_1) = [ -\hbar^2/2m_r (\partial^2/\partial q_1^2) + 1/2 k q_1^2 ] \psi(q_1) \quad (2-7)$$

This equation can be recognized as precisely that of the one-dimensional harmonic oscillator. The energy levels are given by

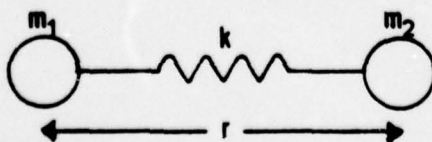
$$E_v = h\nu_0(v + 1/2) , \quad v = 0, 1, 2, \dots \quad (2-8)$$

where  $\nu_0 = (1/2\pi) (k/m_r)^{1/2}$

and  $h$  = Planck's constant. The electric dipole transition selection rules are

$$\Delta v = v(\text{after transition}) - v(\text{before transition}) = \pm 1 \quad (2-9)$$

To determine the rotational contribution to the inherent energy of the diatomic molecule, a non-rigid rotator model must be investigated.





Let

$L$  = angular momentum of the molecule =  $I\omega$

$\omega$  = angular frequency of rotation

$m_r$  = reduced mass

$I$  = moment of inertia =  $m_r r^2$

$k$  = harmonic potential well constant of the molecule

$r_0$  = position of minimum potential energy

The centrifugal force  $F_c$  tending to separate the molecule due to rotational motion is

$$F_c = m_r \omega^2 r \quad (2-10)$$

Since the model is a non-rigid rotator model, the value of  $r$  varies with  $\omega$  and can be determined by equating the centrifugal force to the restoring force assuming a harmonic potential energy function  $k(r-r_0)$ :

$$m_r \omega^2 r = k(r-r_0) \quad (2-11)$$

solving for  $r$  gives

$$r = (kr_0) / (k - m_r \omega^2) \quad (2-12)$$

The kinetic energy for rotation is

$$T = 1/2 I \omega^2 = (L^2 / 2m_r) [ (k - m_r \omega^2) / kr_0 ]^2;$$

expanding

$$T = (L^2 / 2m_r r_0^2) (1 - 2m_r \omega^2 / k + m_r^2 \omega^4 / k^2)$$

and substituting  $\omega = L/I = L/m_r r^2$ ,

$$T = (L^2 / 2m_r r_0^2) [ 1 - (2L^2 / m_r k r^4) + (L^4 / m_r^2 k^2 r^8) ] \quad (2-13)$$

Due to the stretching of the bond, the potential energy term is modified to become:

$$V = 1/2 k (m_r \omega^2 r / k)^2$$

again substituting  $\omega = L/I = L/m_r r^2$

$$V = L^4 / 2k m_r^2 r^6 \quad (2-14)$$

The term  $r$  may be approximated by  $r_0$  and the  $L^6$  term neglected since this model is dealing with only small modifications to the rigid rotor. Therefore, the hamiltonian may be written as a sum of the potential and kinetic energy expressions retaining only terms of fourth or lower order.

$$\mathcal{H} = L^2 / 2m_r r_0^2 - L^4 / 2m_r^2 k r_0^6 \quad (2-15)$$

Operating on the eigenfunctions of the angular momentum operators, the eigenvalues are [12]:

$$E_J = (L^2 / 2m_r r_0^2) (J)(J+1) - (L^4 / 2m_r^2 k r_0^6) (J^2)(J+1)^2 \quad (2-16)$$

where  $J$ =rotational energy level quantum number with the selection rule

$$\Delta J = \pm 1$$

where  $\Delta J = -1$  indicates an energy emission  
 $\Delta J = +1$  indicates an energy absorption.

As a first approximation, the energies given by the rotational energy equation (2-16) and the vibrational energy equation (2-8) may be combined to result in

$$E = h\nu_0 (v + 1/2) + (\hbar^2 / 2m r_0^2) (J)(J+1) - (\hbar^4 / 2m^2 k r_0^6) (J^2)(J+1)^2 \quad (2-17)$$

and simultaneously satisfying the selection rules

$$\Delta J = \pm 1 \text{ and } \Delta V = \pm 1$$

The set of transitions for  $\Delta J = -1$  is called the P-Branch, for  $\Delta J = 0$  (forbidden for the diatomic molecule) is called the Q-Branch, and  $\Delta J = +1$  is called the R-Branch.

The observed values vary slightly from those calculated in (2-17) since higher order deviations and molecular interaction cross terms were ignored. Using equation (2-17) with the known values of  $k$ ,  $r_0$  and  $m_r$ , energy levels can be predicted. Then by using the  $\Delta V = \pm 1$  selection rules, the photon emission transitions can be predicted with the relative intensity of each transition determined by experimental results. Some of the known HF and DF transition wavelengths in the area of interest are listed in Table I [5].

TABLE I. Molecular Transitions of HF and DF

transi- tion	HF wave- length (micro- meter)	relative intensity	transi- tion	DF wave- length (micro- meter)	relative intensity
P <sub>1</sub> (6)	2.7075	0.3	P <sub>1</sub> (9)	3.7155	0.2
P <sub>1</sub> (7)	2.7440	1.0	P <sub>1</sub> (12)	3.8298	
P <sub>1</sub> (8)	2.7830	0.03	P <sub>1</sub> (3)	3.6363	
P <sub>1</sub> (9)	2.8231		P <sub>2</sub> (7)	3.7651	0.5
P <sub>1</sub> (6)	2.8320	0.5	P <sub>2</sub> (8)	3.8007	0.5
P <sub>2</sub> (7)	2.8710	0.2	P <sub>2</sub> (9)	3.8375	1.0
P <sub>2</sub> (8)	2.9110	0.03	P <sub>2</sub> (10)	3.8757	0.2
P <sub>2</sub> (5)	2.9256		P <sub>2</sub> (13)	3.9995	0.3
P <sub>3</sub> (6)	2.9646		P <sub>2</sub> (8)	3.9270	0.1
P <sub>3</sub> (7)	3.0051		P <sub>3</sub> (5)	3.9487	
P <sub>3</sub> (8)	3.0482		P <sub>4</sub> (7)	4.0212	

## B. HF/DF CHEMISTRY

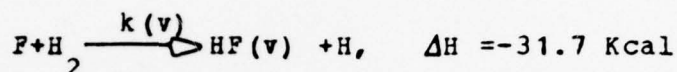
### 1. The Chemical Reaction

The technology of chemical lasers is centered about determining methods for transforming chemical energy into coherent radiation. One aspect of the physics of chemical lasers is the initiation of the chemical process to liberate energy leading to population inversion and eventually to lasing.

In the HF/DF chemical laser, fluorine atoms are normally obtained from the dissociation of one of the gases



$F_2$ ,  $MoF_6$ ,  $SF_6$  or  $NF_3$ . The dissociation takes place when the gases are subjected to processes such as arc heating, DC discharge, flash photolysis, or RF discharge. The dissociated fluorine atoms then flow into the mixing chamber/optical resonator where  $H_2$  is injected into the flow field resulting in the following reaction:



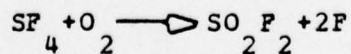
where  $\Delta H$  is the enthalpy of formation and  $k(v)$  is the rate of reaction for the chemical formation of HF molecules in the vibrational level  $v$ . The generation of vibrationally excited molecules in the above reaction results in the first three ( $v=1,2,3$ ) vibration levels being populated with the following ratios [4]:

$$N(2)/N(1) = 5.5$$

$$N(3)/N(2) \geq 0.47$$

The energy imparted to the molecule is partitioned with 57% vibrational, 37% translational, and 6% rotational excitation. Therefore, vibrationally excited molecules in the second level acquire approximately 19 Kcal per mole energy.

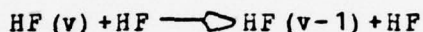
Experimental results [6] indicate that at the maximum laser output power point, the  $SF_6$  is not completely dissociated. Addition of  $O_2$  to the plenum contributes to the heat of combustion and allows more fluorine atoms to be liberated with the reaction



Both sulfur tetrafluoride ( $SF_4$ ) and sulfuryl fluoride ( $SO_2F_2$ ) are non-reactive with glass at room

temperature; however a  $\text{SO}_2\text{F}_2$  reaction with glass begins at 420K [7].  $\text{SF}_4$  and  $\text{SO}_2\text{F}_2$  are water soluble and deposits in the discharge tube can be easily flushed. The addition of  $\text{O}_2$  to the plenum allows for an approximate 20% increase in closed cavity power.

One of the shortcomings of the HF/DF laser is the rapid degradation of the upper vibrational state's population due to collisional self-relaxation resulting in



This degradation is primarily due to a rather short collisional relaxation time of 3 to 4 microseconds [8]. There are at this time two methods by which this quick relaxation or depopulation of the upper states can be slowed down to allow a higher probability of stimulated emission to occur before collisional deactivation takes place.

The first method is to increase the velocity with which the excited HF/DF molecules are drawn past the optical cavity thereby delaying the deactivation to a point further downstream. The second method is to reduce the density of the excited HF/DF molecules in the flow stream to diminish the possibility of molecular collisions. To accomplish this the pressure of the cavity is lowered and an inert gas is mixed with the plenum gas as a diluent. Argon, helium, nitrogen, and xenon have been experimentally successful as diluents but helium [9] was found to allow a 40% increase in peak power output over nitrogen and more over argon and xenon.

## 2. A Qualitative Description of Fluorine and Hydrogen Fluoride

A. Fluorine is known to combine with all elements, with the exception of inert gases in their stable states. With the exception of oxygen, all fluorine combinations are exothermic. Of these exothermic reactions, many are explosive in nature. Fluorine is the most active of all the elements, being extremely reactive with metals, glass, and compounds of most other elements.

Contrary to the general opinion, the homogeneous reaction of molecular fluorine and hydrogen is slow. The reaction is not accelerated by ultraviolet rays or the presence of small amounts of chlorine. The interaction between  $F_2$  and  $H_2$  is a chain reaction which originates on the walls of the container. This process takes place with particular intensity on the surface of quartz (even at 150°K the mixture explodes) [7].

B. Hydrogen fluoride is a tightly bound molecule composed of the most electro-negative atom (fluorine) and the smallest (hydrogen). It has a large dipole moment and takes part in many reactions both as a catalyst and fluorine donor. The liquid phase is strongly associated with a low surface tension but is best known for its ability to etch glass precluding the use of glass in critical work. The liquid is a strong acid and excellent dehydrating agent, but it is impossible to dry HF by chemical means. Because of its hydrogen bonding tendencies HF(gas) forms dimers and multimers readily. It is the most non-ideal gas known, but in the liquid form it is physically similar to water. At room temperature it has a vapor pressure slightly over one

atmosphere, while at liquid nitrogen temperatures it is a solid. It is a good solvent dissolving most of the halide salts readily. In the pure anhydrous form it is a poor conductor, although the addition of impurities such as salts or water produce many ion pairs. HF is also a mild local anesthetic which produces a bad lingering sore if allowed to come in contact with the skin. Unfortunately the sensation of pain does not arise immediately but rather several hours after contact. HF (gas) inhaled with air is retained in the upper respiratory tract attacking the skin and mucous membranes leading to ulcers of the upper tract. Concentrations of 50 to 250 ppm are dangerous even for brief exposures [10].

As can be readily ascertained from the description of fluorine and hydrogen fluoride above, all safety regulations and precautions pertaining to  $F_2$  and HF handling and use must be strictly adhered to for the good of all concerned.

### C. THE OPTICAL RESONATOR

#### 1. Multiline Operation

The optical resonator is the feedback mechanism of the laser and provides for output coupling of the laser power.

The optical resonator under consideration, fig 16, consists of a pair of Brewster windows and mirrors. The laser power is extracted from the laser cavity through the Brewster windows which linearly polarize the output.



Multiple passes through the lasing medium are obtained through the use of the mirrors. The power is extracted from the system by making one of the mirrors partially transmitting. The optimum transmission coefficient for the mirror may be computed [11] to be:

$$T_{opt} = -L_i + [g_0 L_i]^{1/2}$$

where  $L_i$  is the sum of unavoidable residual losses and  $g_0$  is the unsaturated gain. For DF lasers  $T_{opt}$  is less than 10%.  $T_{opt}$  for HF lasers is taken from fig 4 which was provided by J. Beggs of the Aerospace Corporation.

## 2. Single-line Operation

To make the HF/DF Laser a useful tool for the study of atmospheric propagation, it is desirable to be able to select a single line or wavelength for propagation. This may be accomplished through the use of a diffraction grating replacing one of the laser mirrors. A blazed reflection grating with its associated geometry is shown in fig 5. The blazed reflection grating consists of grooves, with flat smooth faces, inclined to the surface at an angle  $\theta_B$ , known as the blaze angle. The wavelength of light for which the direction of reflection from the groove face is the same as the angle of diffraction, for a given angle of incidence, is the blaze wavelength. A grating may be used at the first order diffraction wavelength or the second order of one half this wavelength or the  $m^{th}$  order of one  $m^{th}$  of that wavelength.

The general grating equation is:

$$m\lambda = d(\sin \alpha + \sin \beta)$$

$$m = \dots -1, 0, +1, \dots$$

One application of the blazed reflection grating is using it in a Littrow manner, i.e.  $\alpha = \beta$ : This calls for the rays from the optical cavity to be perpendicular to the groove faces. Incoming rays at the blaze wavelength, one half the blaze wavelength, or one  $m^{\text{th}}$  blaze wavelength will be reflected back into the optical cavity in phase. The general grating equation reduces to:

$$m\lambda = 2d \sin \alpha$$

The grating may be used in this manner to replace the totally reflecting mirror with the output still taken through the partially reflecting mirror. If it is desired to improve the Q of the optical cavity, the grating replaces the partially reflecting mirror and the output is taken from the so called zero order specular reflection. The output is taken at an angle  $\alpha$  with respect to the grating normal, opposite to the input ray, as shown in fig 5. The name zero order specular reflection refers to the fact that rays diffracted from adjacent grooves have a zero path length difference to some point along  $\alpha$ .

It would appear from the mathematical treatment of an ideal grating that the grating would be useful only at a single specified wavelength of the HF/DF laser and many gratings would be required. In reality the grating is not ideal and does not have flat smooth surfaces at a given

blaze angle. The surfaces are somewhat rounded and therefore the grating operates at reduced efficiency over a band of wavelengths. There are certain disadvantages as a result of the fact that the grating operates over a range of wavelengths.

First of all if the imperfections of the grating are too large its efficiency may drop so far that the laser will not operate at any wavelength.

Secondly, the rotation of the grating through an angle  $\Delta\theta$  to select a desired wavelength causes the output beam to rotate through an angle  $2\Delta\theta$ . This adverse effect can be eliminated through the use of an additional output mirror as shown in fig 6. The grating and extra-cavity mirror are turned as a unit about an axis of rotation which contains the intersection of the extended planes of the grating and mirror. A corner cube effect is obtained, maintaining the output beam in a constant direction as the grating is rotated to select the desired wavelength.

### III. THE HF/DF LASER AT THE NAVAL POSTGRADUATE SCHOOL

#### A. EQUIPMENT LOCATION

The HF/DF laser at the Naval Postgraduate School was originally located in the basement of Spanagel Hall. Due to cramped quarters and necessarily long vacuum lines this location was undesirable. Alternative basement locations selected were unacceptable because the noxious effluent gases and potentially dangerous laser output powers present required total environmental isolation.

A rooftop location was finally selected because: 1) The roof location in itself eliminated much of the personnel traffic that is encountered in the basement. 2) The room can be made optically intact and is not served by the central heating and air conditioning of the rest of the building. 3) Long range propagation tests can be conducted to the Coast Guard pier if necessary.

This location was not equipped with the water and electrical services required for the vacuum pump and power supply. These services were installed by the Public Works Department.

Several unique safety features were incorporated in the laser installation of room 609. To ensure the system is not operated by unauthorized personnel a key lock was placed in the electrical supply circuit and must be energized before either the vacuum pump or power supply can be energized.

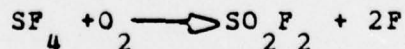


The vacuum pump and power supply have separate circuit breakers and when the one for the power supply is energized a red light outside the entrance to the room automatically begins to flash. Additionally there is a master electrical cutoff switch located outside the room which secures both vacuum pump and power supply. A schematic of the complete electrical system is given in fig 9, while a photograph demonstrating the warning signs posted outside the door is shown as fig 10.

## B. EQUIPMENT DESCRIPTION

### 1. The Laser Bench

The laser at the Naval Postgraduate School is centered around a laser head, fig 11, obtained from the Aerospace Corporation. The source of free fluorine radicals is sulfur hexafluoride. This dictates the construction of the laser head which consists of: a) the discharge tube, b) the mixing chamber, and c) the resonant cavity. A mixture of sulfur hexafluoride, oxygen, and helium is injected into the discharge tube at the end opposite the mixing chamber. The electric discharge through the tube dissociates the sulfur hexafluoride by electron impact. Complete dissociation is not obtained, but oxygen is added and more free fluorine radicals are obtained by the reaction:



Experimental evidence of the impact of  $\text{O}_2$  addition [6] was obtained by Mirels and Spencer.

The discharge tube is made of pyrex glass, 32 mm in diameter, surrounded by a 1 3/4 inch diameter lucite tube. Two discharge tubes were provided, one 12 inches and the other 24 inches in length. A constant flow of water is maintained between the two tubes for cooling. The discharge tube encloses the anode which consists of eight six-inch nickel wire electrodes, each connected to a common high voltage DC power supply through a series 200k ohm ballast resistor. The ballast resistors are forced air cooled. They are pictured under the laser bench in fig 12. The cathode is copper and also serves as the interface between the discharge tube and mixing chamber.

The fluorine atoms are then focussed into a broad shallow region by a fan shaped nozzle at the input to the mixing chamber, figs 14 and 15. The hydrogen or deuterium is injected perpendicular to the gas flow from above and below through a single line of jets. The chemical reaction takes place in this mixing region forming the vibrationally excited HF/DF molecules. The resonant optical cavity is placed transverse to the gas flow, downstream from the injection point, at the point of maximum optical gain. The output is coupled from the cavity by means of a pair of Brewster windows which can be positioned longitudinally for maximum gain. Two interchangeable pairs of Brewster windows, one BaF<sub>2</sub> (0.25 - 15  $\mu$ m transmitting), and the other sapphire (0.14 - 6.5  $\mu$ m transmitting), were provided by the Aerospace Corporation. For multiline DF operation the optical resonator, fig 16, is formed by a 100% broadband reflecting mirror (200 cm radius of curvature) and a 90% reflecting mirror from 3.6 - 4.0 micrometer (300 centimeter radius of curvature) spaced with a Burleigh four-bar system using precision mirror mounts. For multiline operation at HF wavelengths the same 100% broadband mirror is utilized but a mirror of 85% or 95% reflectance from 2.6 - 3.0 micrometers

replaces the 3.6 - 4.0 micrometers mirror. When in multiline operation the following parameters are set and indicated in fig 17:

$$R_1 = -300 \text{ cm} = \text{radius of mirror one}$$

$$R_2 = 200 \text{ cm} = \text{radius of mirror two}$$

$$L = 34.29 \text{ cm} = \text{optical resonator length}$$

Mirror curvature is taken as positive when the center of curvature is to the left of the mirror. The stability of this confocal cavity is checked by the following criterion [11]:

$$0 \geq (1 - d/R_1) (1 - d/R_2) \geq -1$$

For the multiline configuration of this laser the stability parameter is 0.73. More can be learned about the optical resonator by calculating the following quantities. The Rayleigh range, the range when the area of the beam doubles from its minimum value, can be calculated to be [11]:

$$z_0 = \left[ \frac{L(-R_1 - L)(R_2 - L)(R_2 - R_1 - L)}{(R_2 - R_1 - 2L)^2} \right]^{1/2} \\ = 61.46 \text{ cm}$$

The Rayleigh range will be used to find subsequent beam parameters. The corresponding minimum beam size is given by the following equation [11]:

$$w_0 = [z_0 \lambda / \pi n]^{1/2}$$

which is 0.74 millimeters for HF wavelengths and 0.865 millimeters for DF wavelengths.

The minimum beam size is much less than the minimum cavity dimension of two millimeters so the beam can be focussed through the cavity without fear of diffraction. To complete the picture of the optical resonator it is necessary to find  $z_1$  or  $z_2$ , the distance from the center to mirror 1 or 2, given by [11]:

$$z_i = 1/2 [R_i + (R_i^2 - 4z_0^2)^{1/2}]$$

$$z_1 = -13.39 \text{ cm}$$

$$z_2 = +20.90 \text{ cm}$$

$z = 0$  is the location of the minimum spot size.

For single-line operation with this laser system, the partially reflecting mirror is replaced by a diffraction grating from PTR Optics Company. Catalog number ML 501 is used for HF wavelengths while ML 601 is used for DF wavelengths. Both are ruled with 300 grooves/millimeter. The blaze wavelengths are 2.8 micrometer (blaze angle 24.8 degrees) and 3.5 micrometer (blaze angle 31.7 degrees). Their efficiency at rated wavelength is 92%. For a constant angular output as discussed in the theory section of this



report, it was necessary to design a miniature spectrometer table which could be mounted in the Burleigh mirror mount provided. The resultant diffraction grating mount, built by Bob Moeller, is shown in fig 7. The flat mirror on the mount was acquired from Edmund Scientific Supply.

The corresponding beam parameters for the optical resonator with the diffraction grating and the 100% reflecting mirror are as follows:

$$z_0 = 75.38 \text{ cm}$$

$$w_0(\text{HF}) = 0.819 \text{ mm}$$

$$w_0(\text{DF}) = 0.95 \text{ mm}$$

$$z_1 = 0$$

$$z_2 = L = 34.29$$

The unperturbed beam radius as a function of range is given by:

$$w(z) = w_0 \left( 1 + z/z_0 \right)^{1/2}$$

This function is plotted for a DF single-line optical resonator in fig 26.

The laser head was delivered by Aerospace Corporation mounted on a bench which was complete with a chamber pressure gauge, Rotometer gas flow meters and valves, leveling jacks, and coolant water valves, as pictured in figs 12 and 23.

## 2. Laser Support Systems

Six support systems were required to complete the laser system designed around the laser head. They were the gas supply system, water cooling system, DC power supply, vacuum system, scrubber system, and detector system.

### a. Gas Supply System

As previously described a laser bench was provided complete with gas flow meters and valves. The only equipment in the gas supply system external to the laser bench was the gas regulators and gas bottles. The necessary gases are: a) sulfur hexafluoride and oxygen for generation of fluorine radicals, b) helium as a diluent gas as described earlier in the theory section, c) hydrogen or deuterium injected into the mixing chamber for HF/DF molecule generation. The gas bottles were connected through their appropriate regulators to the laser bench with 1/4 inch copper tubing. Gases may be obtained as described in appendix A.

### b. Water Cooling System

As provided, the laser bench had separate coolant connections for the chamber and discharge tube. At the Naval Postgraduate School these systems were connected

in parallel to a single 500 gallon per hour pump. This submersible pump is in a 25 gallon distilled water reservoir equipped with a thermometer so that the operator can monitor for dramatic temperature increases. Care was taken to bleed all air from the coolant system so that hot spots are not formed on the electric discharge tube.

### c. DC Power Supply

The laser head was previously operated at the Aerospace Corporation with a power supply which could supply 14 kilovolts at 250 milliamps. This supply was not specifically optimized for the laser head, but it did provide single-line laser output of 250 milliwatts in the

P<sub>2</sub> (8) transition of DF, exceeding the design specifications.

A power supply on loan from the Lockheed Research Laboratories, obtained by Jim Cook, was used for initial laser operation. It was adapted for DC operation by bypassing the input SCR's. An attempt to adjust the supply voltage with an input rheostat failed due to high input currents. Filtering for this supply was provided by four 10 kilovolt, 100 microfarad capacitors connected in series. Calculated ripple was less than one percent. These capacitors weighed approximately 400 pounds and occupied a cabinet 3 ft x 3 ft x 3 ft. These capacitors in addition to the power supply made the electrical system excessively massive for portable use.

Although the laser did not operate with this supply (10 minutes of experimental time), it is believed it would have been adequate since a lasing threshold was obtained (15.5 kilovolts at 440 milliamps). Regretably since this supply was not designed for DC operation, it proved to be quite inadequate. For a 7.5 kilowatt output it

required an input of 43.5 kilowatts. During initial operation a solder joint on one of the ballast resistors opened apparently causing a surge to the power supply. The subsequent damage resulted in an inoperative power supply with all of its rectifying diodes shorted. Due to the high cost of replacement diodes and the inefficiency of this power supply it was decided a replacement power supply was required. Fortunately funds became available for purchase through normal channels of a Hipotronics Model 820-500, 20kV, 1/2 ampere DC supply, fig 18. With 5% ripple from the supply the capacitor bank was eliminated.

#### d. Vacuum System

The laser head was operated during pre-delivery check-out at a cavity discharge pressure of 8 torr at a flow rate of 5 liter/sec. Subsequent conversations with Mr. Jim Beggs of Aerospace Corporation indicate they now operate their four inch cavities at 13 torr and 39 liter/sec (82 cfm) with a much larger power out. An available water-cooled vacuum pump, a KDH-130, fig 20, having a capacity of 134 cfm (62 liters/sec) was installed outside the laser room reducing the noise level in the laser room. Approximately six feet of three inch copper line connects the vacuum pump to the scrubber described in the next section. The scrubber in turn is connected to the discharge outlet of the cavity by five feet of 1 1/2 inch copper line. These additional restrictions dictate a pump requirement of greater than 39 liters/sec. The KDH-130 easily met the pumping requirement maintaining a cavity pressure of 3 torr at the higher gas flow rates. A schematic of the entire vacuum system is shown in fig 19.



#### e. Scrubber System

The noxious nature of the laser effluent gases demands that a method be devised to filter out the HF or DF. With the thought of making this laser system portable it was decided the lye bubbler system previously used must be replaced. The basic principle of the present system is that the effluent gases are passed over a basic compound which neutralizes them. The present system was modeled after a scrubber at the Air Force Weapons Laboratory, Kirtland AFB, New Mexico. The plans were modified to accomodate larger gas flow rates. Actual construction of the scrubber was accomplished by MR1 Adams of the Naval Postgraduate School Machine Shop. Adapters were fashioned for the inlet and outlet of the scrubber box by Bob Moeller. These adapters allowed o-ring seals with the inlet and outlet pipes. A detailed view of the scrubber is given in figs 21 and 22. By staggering the position of the drawers as shown the effluent gases must pass over a large area of basic compound which in this scrubber is soda lime contained in the screened drawers. When the soda lime is neutralized to the point that it is no longer effective it will change color to purple. The scrubber was opened after each eight hours of operation to check the condition of the soda lime.

The scrubber was placed in the vacuum system before the vacuum pump to protect the pump oil. In similar systems it was found that pump oil absorbed more of the noxious gases than the scrubber when the scrubber was located after the pump. With the scrubber located before the pump it is necessary to check the oil only ocasionaly with litmus paper for contamination. Contaminated pump oil results in excessive pump wear. Contaminated oil was delivered to the fire department for disposal. The

neutralized soda lime is harmless and may be disposed of in any convenient manner.

f. Detector System

Detection of infrared radiation at the fixed laser location was accomplished with a SCIENTECH 362 power/energy meter. The 362 is a wide-range instrument capable of detecting laser powers from one milliwatt to ten watts with a maximum permissible energy density of 200 watts/cm<sup>2</sup>. These features made it an ideal instrument for detection of both the single-line and multiline outputs of the HF/DF laser.

For the study of atmospheric propagation it is anticipated the DF single-line output will be utilized at an average line power of 100 milliwatts at P<sub>2</sub>(8). Detection will be accomplished with a nitrogen-cooled photovoltaic Indium Antimonide detector obtained from Santa Barbara Research Co. This detector has a nominal sensitivity of 2 microwatts cm<sup>-2</sup>. The detector is configured to be mounted in the eighteen inch telescope of the Naval Postgraduate School Mobile Optical Lab.

## C. EQUIPMENT OPERATION

### 1. Multiline Alignment Procedure

To ensure proper alignment of the HF/DF laser in both single-line and multiline operation, the laser must be operated with all nominal gas flows on and discharge current at the desired range. This will allow the hydrogen-fluorine flame, fig 24, in the optical cavity to be observed and thus will indicate where the mirrors  $M_1$  and  $M_2$  should be aligned.

After observing the location of the hydrogen-fluorine flame (about 1.5 mm downstream of the hydrogen injection nozzles), set up a He-Ne (6328Å) alignment laser and beamsplitter (microscope glass slide) as indicated in Fig 25. Place a piece of white paper in front of  $M_2$  and adjust the beamsplitter and alignment laser beam so that it passes through the cavity unobstructed in the flame position determined earlier.

After positioning the beam through the cavity, remove the paper from  $M_2$  and adjust  $M_2$  to reflect the beam back through the cavity at the flame location. If the reflected beam on  $M_1$  can not be located place a white paper in front of  $M_1$ . When the beam has been optimized on  $M_1$ , remove the paper and adjust  $M_1$  to reflect the beam back

through the cavity and strike  $M_2$  in the same position that the original beam was incident upon  $M_2$ . This portion of the alignment is critical and must be precise to within 0.8 mm for lasing to occur. It may be aided by placing an index card with a 1.0 mm hole in it between the Brewster window and  $M_2$  with the original beam going through the hole and adjusting  $M_1$  until the reflected beam is incident on the hole. The laser is now aligned.

The entire alignment procedure depends on the proper positioning of the transverse alignment beam through the point where the hydrogen-fluorine flame contains vibrationally excited HF/DF molecules.

## 2. Single-Line Alignment and Operation

For single-line operation the proper grating for DF or HF operation is mounted on the grating table and this unit is placed in the Burleigh mirror mount as shown in fig 13. Before securing the diffraction grating mount in place it is necessary to place its spectrometer table as near to horizontal as possible (this is checked later in the alignment procedure).

Equipment setup for single-line optical alignment, fig 25, is the same as for multiline optical alignment with the diffraction grating replacing mirror  $M_2$ . The beam is positioned in the cavity in the same manner as in multiline alignment. The visible alignment laser produces several orders of diffraction. The brightest order should be aligned back down the cavity using the grating tuning and



vertical micrometer adjustments. With use of the grating tuning micrometer it should be possible to reflect the other orders through the cavity without tuning the vertical micrometer. If it is not possible it will be necessary to relevel the grating mount and repeat the above alignment. If the multiline alignment has been previously completed no adjustment of mirror  $M_1$  should be necessary; otherwise the mirror is adjusted as in the multiline section.

The alignment of the optical cavity is complete at this point and subsequent adjustments are necessary only to select the desired wavelength (line) for propagation.

The horizontal micrometer on the grating end is set to 2.89; then the desired wavelength is selected with the grating tuner in accordance with Table II. Slight fine tuning will be necessary due to the inherent instability of the hydrogen-fluorine flame.

### 3. Laser Start-up and Shut-down Procedures

Laser start-up and shut-down should be conducted with the checksheets provided as appendices B and C, respectively.

TABLE II.

## Single-line Selection Settings

HF			DF		
Trans- ition	Angle (Degrees)	Micro- meter	Trans- ition	Angle (Degrees)	Micro- meter
P <sub>1</sub> (4)	23.2	4.04	P <sub>1</sub> (5)	32.4	2.45
P <sub>1</sub> (5)	23.6	3.99	P <sub>1</sub> (6)	32.8	2.39
P <sub>1</sub> (6)	24.0	3.88	P <sub>1</sub> (7)	33.2	2.335
P <sub>1</sub> (7)	24.3	3.82	P <sub>1</sub> (4)	33.4	2.295
P <sub>1</sub> (8)	24.7	3.76	P <sub>2</sub> (8)	33.5	2.27
P <sub>2</sub> (2)	23.8	3.93	P <sub>1</sub> (5)	33.7	2.245
P <sub>2</sub> (3)	24.1	3.85	P <sub>2</sub> (9)	33.9	2.21
P <sub>2</sub> (4)	24.5	3.80	P <sub>1</sub> (6)	34.0	2.18
P <sub>2</sub> (5)	24.8	3.74	P <sub>2</sub> (10)	34.2	2.145
P <sub>2</sub> (6)	25.1	3.69	P <sub>1</sub> (7)	34.4	2.12
P <sub>2</sub> (7)	25.5	3.62	P <sub>2</sub> (11)	34.6	2.07
P <sub>2</sub> (8)	25.9	3.55	P <sub>1</sub> (8)	34.8	2.055
P <sub>3</sub> (6)	26.4	3.48	P <sub>2</sub> (9)	35.1	1.99
P <sub>3</sub> (7)	26.8	3.40	P <sub>2</sub> (10)	35.5	1.915
P <sub>3</sub> (8)	27.2	3.32	P <sub>2</sub> (11)	36.0	1.84
			P <sub>2</sub> (12)	36.4	1.77
			P <sub>2</sub> (10)	36.9	1.685
			P <sub>3</sub> (11)	37.3	1.60

#### D. LASER PERFORMANCE

The HF/DF laser at the Naval Postgraduate School exceeded initial anticipated performance parameters by achieving 160 milliwatts of laser power in the  $P_2(8)$  DF transition. Additionally the laser has performed well in all four modes of operation: 1) HF multiline, 2) HF single-line, 3) DF multiline, and 4) DF single-line. An account of laser performance in each mode of operation follows. All performance tests were conducted with the 24 inch discharge tube.

##### 1. HF Performance

###### a. Multiline Performance

On 1 April 1977, lasing action in the HF mode was achieved with a multiline power out of about 40 milliwatts using the 95% reflectance (R) three meter radius of curvature mirror as the output coupler and a 100% R two meter radius of curvature mirror as the total reflector. Although this was a minimal output, through fine tuning of the optical cavity, optimization of the gas flows, discharge current and cavity pressure, a quantum increase in the power out was expected.

Optimization of the above parameters resulted in 750 milliwatts of multiline output power on 7 April 1977. Subsequent phone conversations with Mr. Jim Beggs of Aerospace Corporation on 11 April 1977 indicated that a

sizable increase in HF multiline output power may be obtained by: 1) using an 85% R output coupler mirror as indicated in fig 4. 2) unsoldering the cavity and milling out the cooling vanes downstream from the hydrogen injection nozzles. Mr. Beggs indicated the latter suggestion came about because of suspected reflected turbulent pressure gradients caused by the vanes.

An 85% R three meter radius of curvature mirror was ordered and received from Valtec Company of Holliston, MA. The cavity was unsoldered and the cooling vanes were removed by milling. The mixing chamber before and after the milling is shown in fig 15.

The laser was reassembled and with flow parameters that previously resulted in 750 milliwatts (cavity with vanes), a maximum power of 1.6 watts was obtained. The 95% R output coupling mirror was then replaced with the 85% R mirror. Subsequent efforts at maximization resulted in four watts power out.

The 100% R two meter mirror was then replaced with an optical quartz flat with a 1500 angstrom aluminum coating deposited on it. Use of the 85% R mirror and the quartz flat resulted in a power out of three watts.

Returning to the confocal cavity arrangement with the 85% R output coupler optimization studies were then conducted with the results in figs 27, 28, 29, and 30.

The multiline HF optimization results indicate that the addition of oxygen and helium to the gas flow only act as auxiliaries to the fuel and oxidizer. With oxygen at zero flow, lasing at 30% of full power was achieved. A threefold increase in the laser power was obtained with the addition of oxygen because of the increase in fluorine



radicals as discussed in the theory section. Zero flow helium operation could not be obtained due to a current limit dictated by the power supply; however, with an increase of the mass flow of helium from 0.025 to 0.05 grams/sec a 74% increase in laser power was achieved. The optimization of sulfur hexafluoride and hydrogen provided data with peaks at the optimum flow rates when the fuel and oxidizer were balanced. The power input and the chemistry of the reaction indicates that complete dissociation of the sulfur hexafluoride is highly unlikely. This fact along with increased collisional deactivation at higher mass flow rates allows an optimum peak power to be obtained by use of the data shown in figs 27, 28, 29, and 30.

The resulting optimized multiline power out was 6.5 watts with mass flows as follows:

$$\text{SF}_6 = 0.600 \text{ grams/sec}$$

$$\text{O}_2 = 0.182 \text{ grams/sec}$$

$$\text{H}_2 = 0.019 \text{ grams/sec}$$

$$\text{He} = 0.053 \text{ grams/sec}$$

The 6.5 watts of laser power had amplitude fluctuations of less than one percent.

#### b. Single-line Performance

Using the tunable single-line adapter as shown in fig 7 with the PTR ML 501 reflection grating fifteen individual HF lasing transitions were obtained. Fig 31 gives the lines that were measured with their relative intensities, transitions involved, and the wavelengths.

The peak power out for the individual lines varied from the  $P_1(7)$  line at 600 milliwatts to the  $P_3(8)$  line at 90 milliwatts. The data agree with published results under similar conditions by Spencer, Beggs, and Mirels [13].

In the single-line output mode it was observed that the mode and amplitude stability were greatly enhanced from that of multiline operation. This is thought to have come about from the case that in the multiline mode of operation the population inversion for a few vibrational states is at or near threshold. If this is the case then in multiline operations there are contributing power and mode transitions that are intermittently lasing thereby causing fluctuations. Conversely in the single-line case, the amplitude and mode fluctuations are minimal. The amplitude fluctuation is than one percent and mode as observed on the thermal image plates was TEM<sub>00</sub>.

A PTR ML 601 reflection grating was received for single-line studies in the DF mode. Upon examination of the efficiencies over the bandwidths of HF and DF it was noted that the ML 601 had an efficiency of 80% at 2.5 micrometers and increased to 90% at 3.0 micrometers. Single-line lasing was attempted and achieved in the HF mode with the ML 601 grating resulting in the measurement of fourteen lines with a maximum power on a single line of 650 milliwatts at 2.8318 micrometers, the  $P_2(6)$  transition. It is felt that the shift in the strong line power resulted from the variation in efficiency from 80 to 90% and that the  $P_2(6)$  line which was previously suppressed somewhat was enhanced by occurring at the grating efficiency corresponding to optimum output

coupling. Fig 4 shows the plot of power out versus transmission for the HF mode (fig 4 courtesy of J.A. Beggs of Aerospace Corp.).

## 2. DF Performance

### a. Multiline Performance

On 15 April 1977, lasing was obtained in the DF multiline mode using a 90% R three meter radius of curvature mirror as the output coupler and a 100% R two meter radius of curvature mirror as the total reflector. The total laser power achieved was 2.5 watts with the following mass flows

$$\begin{aligned}SF_6 &= 0.680 \text{ grams/sec} \\He &= 0.063 \text{ grams/sec} \\O_2 &= 0.270 \text{ grams/sec} \\D_2 &= 0.043 \text{ grams/sec}\end{aligned}$$

and input current of 300 milliamps at 17.5 kilovolts.

Optimization of gas flows in the DF multiline mode were then conducted with the results shown in figs 27, 28, 29, and 30. The maximum optimized multiline laser power that was observed was 3.0 watts using the same mirror configuration described above. The mass flows for gas inputs for the optimized 2.5 watts output were

$$\begin{aligned}SF_6 &= 0.371 \text{ grams/sec} \\He &= 0.038 \text{ grams/sec} \\O_2 &= 0.168 \text{ grams/sec}\end{aligned}$$

$$D_2 = 0.020 \text{ grams/sec}$$

with the input current of 350 milliamps at 17.5 kilovolts. The 2.5 watts output power was the resultant of trade-offs of gas flows and input power. It was determined during optimization that any increase in gas flows or input current up to the maximum allowable by equipment constraints would only increase the output power by 20%.

Comparison of the optimization curves for HF and DF oxygen and helium variation indicated that both oxygen and helium because of the lack of zero flow laser power out are a necessary addition to the DF gas flow whereas with HF they were merely auxiliaries that enhanced the laser power output. This effect is not in agreement with test results reported by Spencer, Beggs, and Mirels [13]. The results for deuterium and sulfur hexafluoride agree for both HF and DF.

#### b. Single-line Performance

In the DF single-line mode of operation, the single-line adaptor as shown in fig 7 was mounted in the optical cavity arrangement as shown in fig 8 with the PTR ML 501 reflection grating having an efficiency of about 84% in the 3.5 to 4.1 micrometer region. Single-line output was achieved with a total of fourteen laser transition lines obtained with a maximum power on a single line of 220 milliwatts at 3.8757 micrometers, the  $P_2(10)$  transition.

Subsequent refinement of the single-line tuning procedures resulted in a total of fifteen lines observed with the maximum power on a single line of 240 milliwatts at 3.8757 micrometers.



Upon receipt of a PTR ML 601 reflection grating with an efficiency at the DF wavelengths of 91%, DF single-line measurements were taken resulting in a total of eighteen lines being detected with a maximum single-line output power of 100 milliwatts at 3.8757 micrometers.

The power output in the DF single-line mode using the ML 601 did not reach the level attained with the ML 501 but it is thought that this is probably due to a misalignment of the grating on the grating mount.

The eighteen lines detected with the ML 601 grating correlated precisely with those reported by Spencer, Beggs, and Mirels [13]. Fig 32 illustrates the results of the single-line measurements using the ML 601 reflection grating and their relative intensities. The DF lines as with the HF lines were amplitude stable to within one percent in the TEM<sub>00</sub> mode.

The power output for the P<sub>2</sub>(8) transition at 3.8007 micrometers for the ML 501 grating was 160 milliwatts optimized and for the ML 601 grating was 75 milliwatts. These power levels appear to be sufficient to allow the ongoing Atmospheric Propagation studies at the Naval Postgraduate School to gather marine boundary layer propagation data at 3.8007 micrometers.

### 3. Portable Performance Study

Initial tests were conducted to determine the feasibility of making the HP/DF laser at the Naval Postgraduate School portable or semiportable to the extent that it could easily be transported to another fixed location. The study was aimed at minimizing: 1) weight, 2) volume, and 3) input power.

The major contributors to the weight, volume, and input power requirement of the fixed location laser were the vacuum pump and power supply. Accordingly these items were the object of the study.

The input power requirement is three-phase 208/220 volts for both the vacuum pump and power supply at the fixed location. All available power supplies with a 20kV capability utilize this three-phase input, therefore establishing a portion of the portable generator requirement. This did not present a problem since a portable 15 kW diesel driven generator with a three-phase capability was readily available. The combined power requirement for the Kinney KDH-130 vacuum pump and Hipotronics Model 820-500 power supply was 10 kW at normal operating loads and therefore no change of the fixed location setup would be required from a power viewpoint to make the system portable. The next step was to look at the possibility of reducing the weight and volume of the system.

After further study it was decided that it would not be economically feasible to replace the power supply since little would be gained. The laser with the 24 inch discharge tube requires a power supply with a minimum capability of 15 kV at 250 mA. Supplies capable of greater

than 12.5 kV have a separate oil-insulated transformer section implying two separate units. If a change in power supply is deemed necessary at a later date the 12 inch discharge tube could be used with 50 kilohm ballast resistors and a 10 kV air-insulated power supply. This smaller power supply would result in a weight reduction of 350 pounds from the present 900 pounds but no volume reduction from 24 ft<sup>3</sup>.

A change in vacuum pump from the 800 pound, water-cooled Kinney KDH-130 to a smaller air-cooled pump would be feasible and necessary. Lasing was attempted and obtained with a Kinney KDH-30 vacuum pump. The pump, capable of 33 cfm, could not maintain a stable vacuum to support 50 milliwatts of P<sub>1</sub> (7) HF lasing. Even less power would have been obtained in the DF mode making it unsatisfactory for propagation studies. Tests conducted by throttling the KDH-130 indicate the minimum feasible pump size would be 50 cfm while 75 cfm would be preferable. The Kinney KDH-65 (69 cfm) and KDH-80 (83 cfm) are air-cooled with a weight of approximately 500 pounds. These pumps come with their own trailers or they could be mounted on the diesel generator trailer to minimize vibration at the laser bench. The laser bench, gas bottles, and power supply would be located in an available 2 1/2 ton van.

It is anticipated that a KDH-80 pump will support flow rates at a vacuum to maintain 100 milliwatts of P<sub>2</sub> (8) DF lasing.

## APPENDIX A

### LASER SUPPLIES

This laser requires four gases for operation. They are  $\text{SF}_6$ , He,  $\text{O}_2$ , and  $\text{H}_2$  or  $\text{D}_2$ . Standard (1A size) bottles were used for all gases. Sulfur hexafluoride was obtained from Matheson Gas Products for \$330. Helium diluent and oxygen are available at the Naval Postgraduate School. For HF operation, commercially available hydrogen stocked at the Naval Postgraduate School can be used; for DF operation, commercially available deuterium is prohibitively expensive. It was found that the Air Force stocks deuterium and will supply a military activity at a reasonable price of \$300 per bottle.

Orders for deuterium are to be sent with MIPR number to:

San Antonio A.L.C.  
Service S.F.S.C.  
Kelly A.F.B. 78241

Expendable deuterium bottles should be shipped to:  
Union Carbide Corp. Y 12 Plant  
Oak Ridge, Tenn. 37830

Soda lime (37 pounds) for the laser scrubber system is available from VWR Scientific at a price of \$65.



## APPENDIX B

### START UP PROCEDURES

1. Turn vacuum pump coolant water on.
2. Insert key into security lock and energize.
3. Energize vacuum pump.
4. Open scrubber vacuum roughing valve slowly.
5. Open all gas cylinder valves at the regulators.
6. Energize ballast resistor coolant fan and cavity coolant pump.
7. Energize high-voltage power supply.
8. Apply high voltage to discharge tube.
9. Turn on He to desired flow rate.
10. Turn on SF<sub>6</sub> to desired flow rate slowly.
11. Turn on O<sub>2</sub> to desired flow rate.
12. Turn on H<sub>2</sub>/D<sub>2</sub> to desired flow rate.
13. Vary cavity vacuum roughing valve to desired pressure.

## APPENDIX C

### SHUT DOWN PROCEDURES

1. Secure high voltage.
2. Close  $H_2$ ,  $O_2$ , and  $SF_6$  gas cylinder regulator valves.
3. Close He flow valve on gas control panel.
4. Pump down  $H_2$ ,  $O_2$ , and  $SF_6$  to clear lines.
5. When lines have cleared secure scrubber vacuum roughing valve.
6. Open He flow valve to fill cavity up to one atmosphere He. (relief valve on vacuum gauge opens at 15 psi)
7. Secure He gas cylinder regulator valve.
8. Allow about five minutes to cool down ballast resistors and cavity coolant water.
9. Secure ballast resistor coolant fan and cavity coolant pump.
10. Secure vacuum pump power.
11. Turn off vacuum pump coolant water.
12. Turn security lock to off position and remove key.

# APPENDIX D

## FIGURES

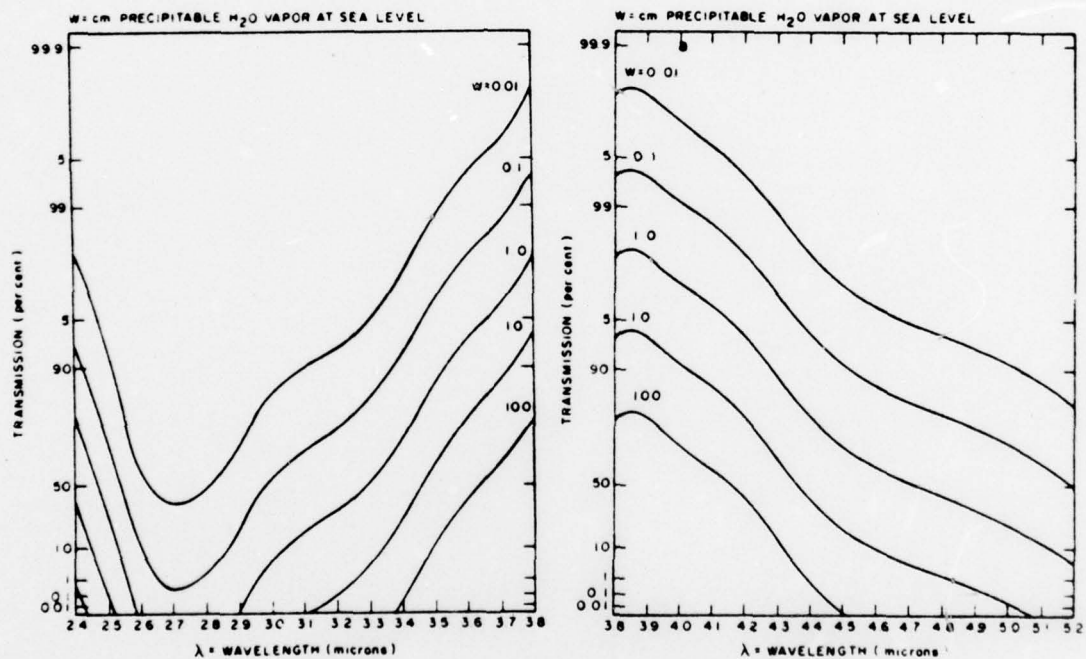


Figure 1 - WATER VAPOR TRANSMISSION(2.4-5.2 Micrometers)

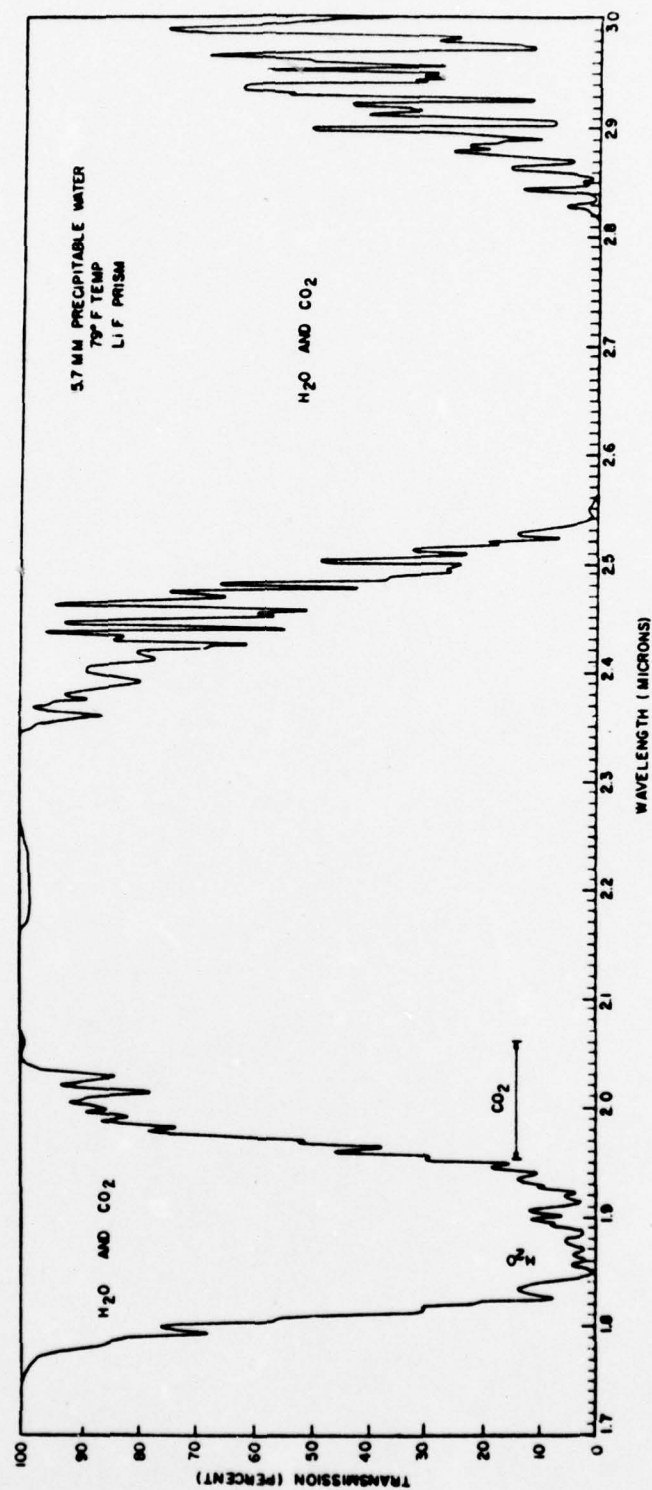


Figure 2 - ATMOSPHERIC TRANSMISSION(1.7-3.0 Micrometers)



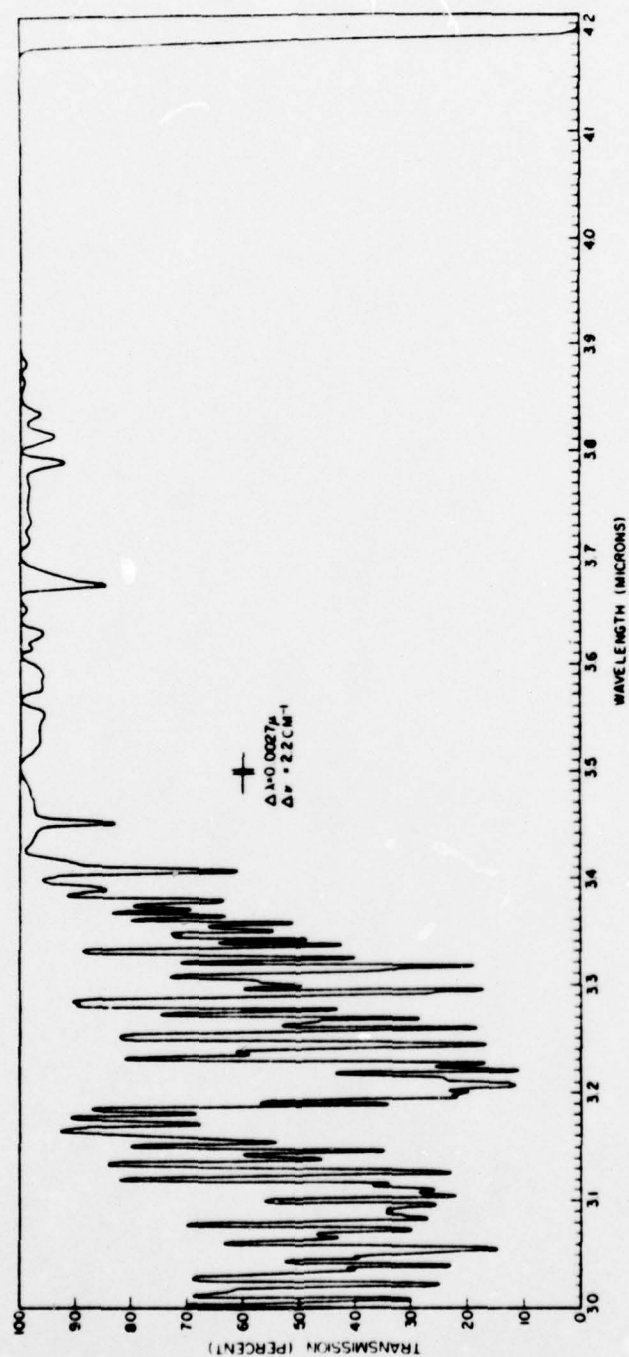


Figure 3 - ATMOSPHERIC TRANSMISSION (3.0-4.2 Micrometers)

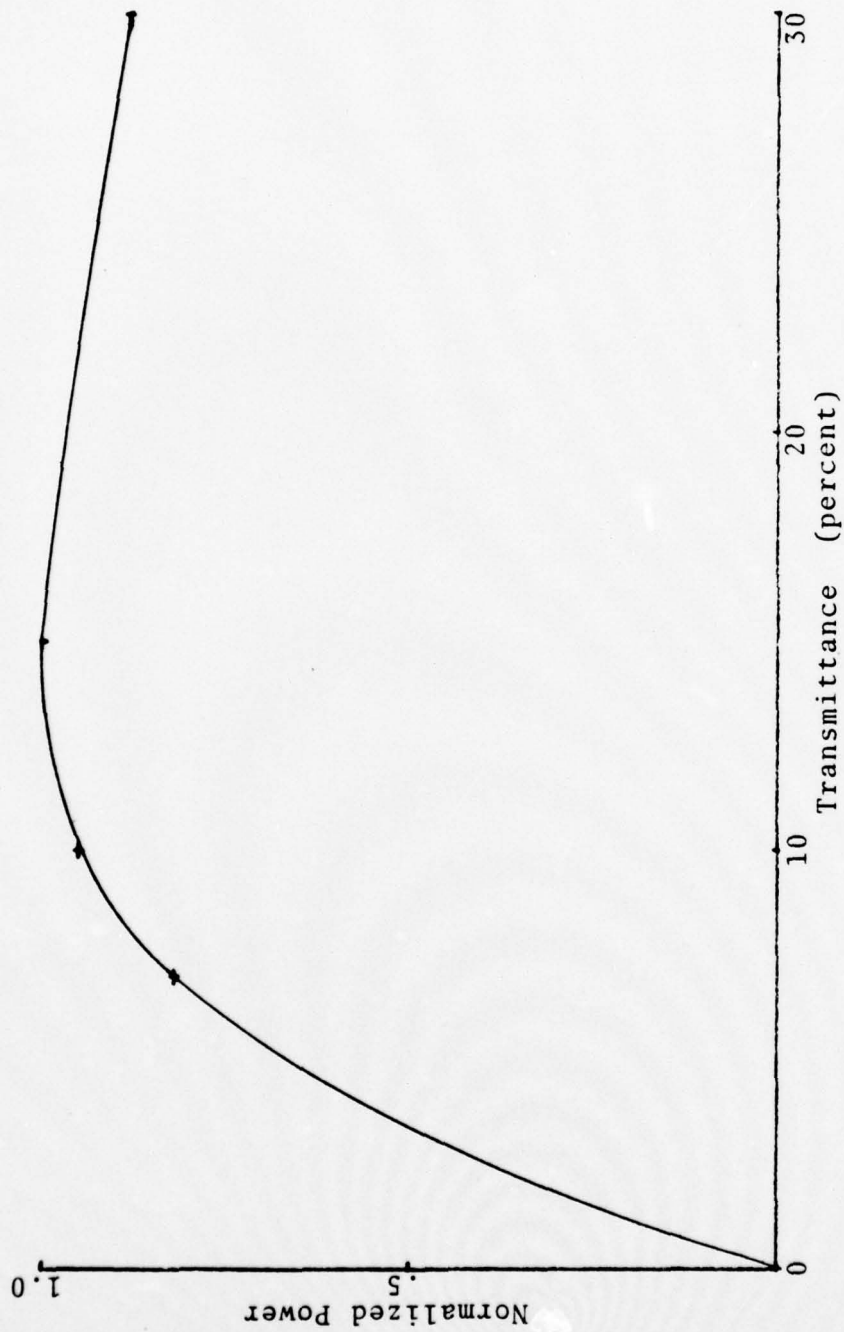


Figure 4 - POWER OUT VERSUS TRANSMISSION COEFFICIENT (HP)

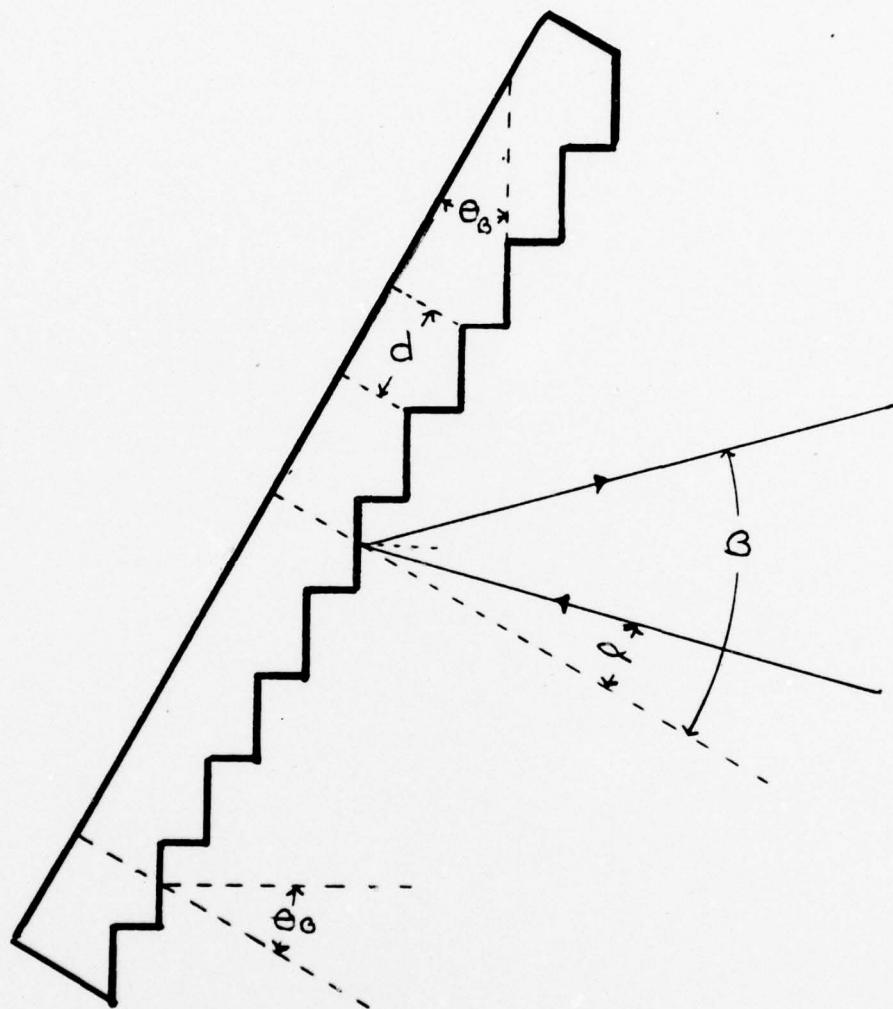


Figure 5 - THE DIFFRACTION GRATING

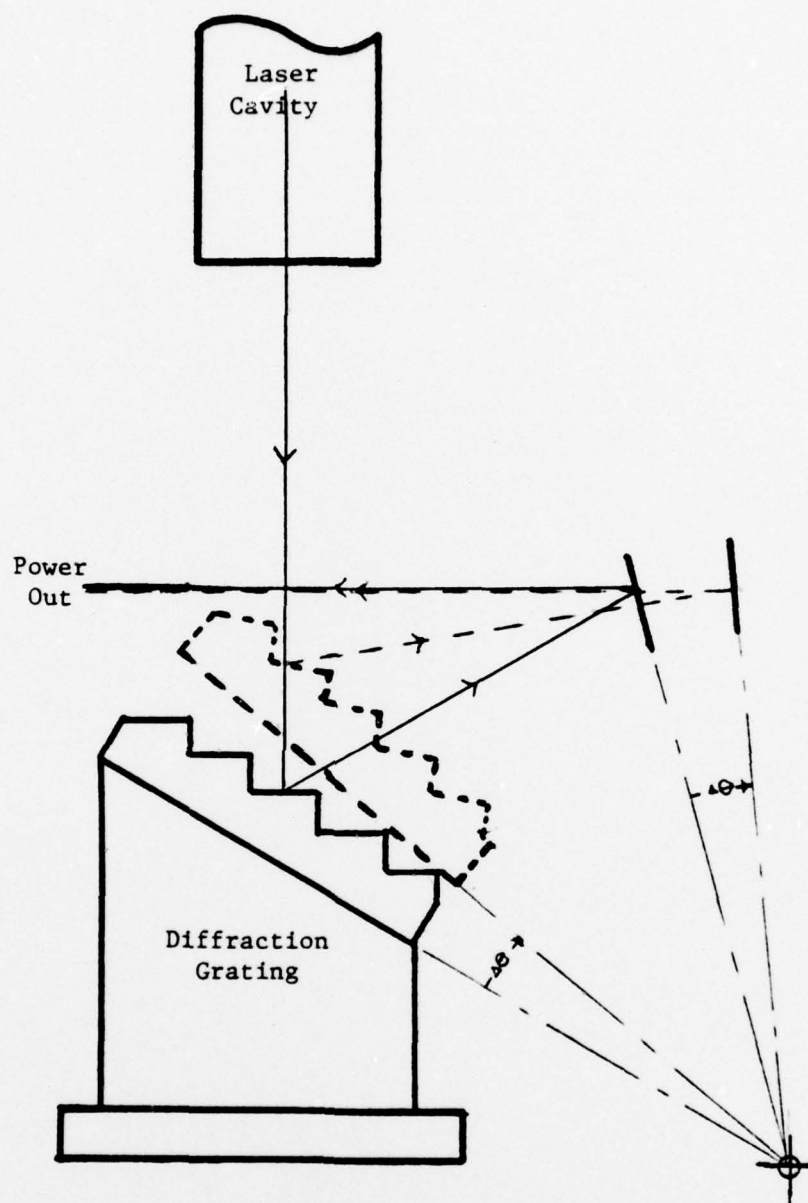


Figure 6 - TUNABLE SINGLE-LINE DIAGRAM



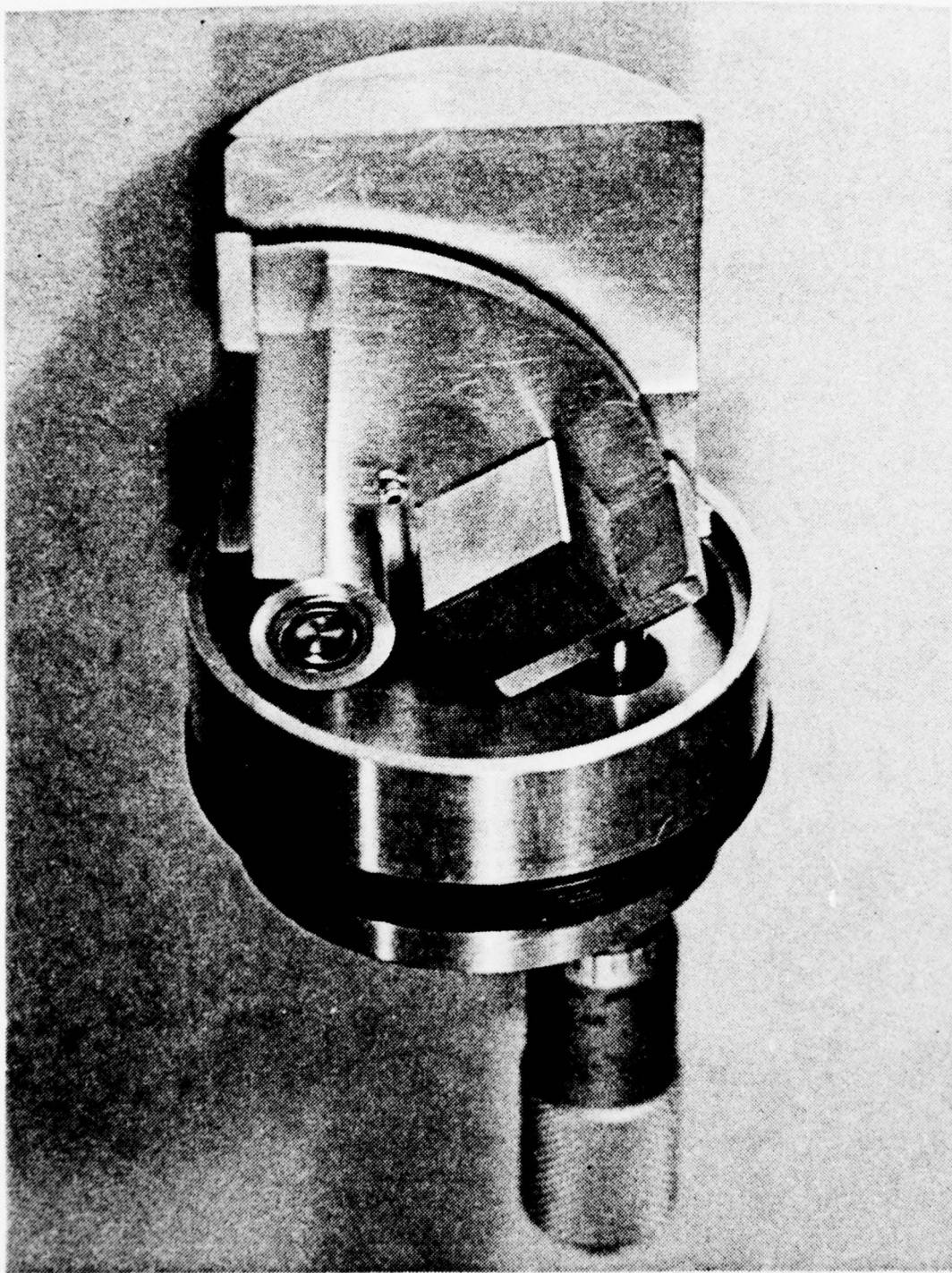


Figure 7 - TUNABLE SINGLE-LINE ADAPTER

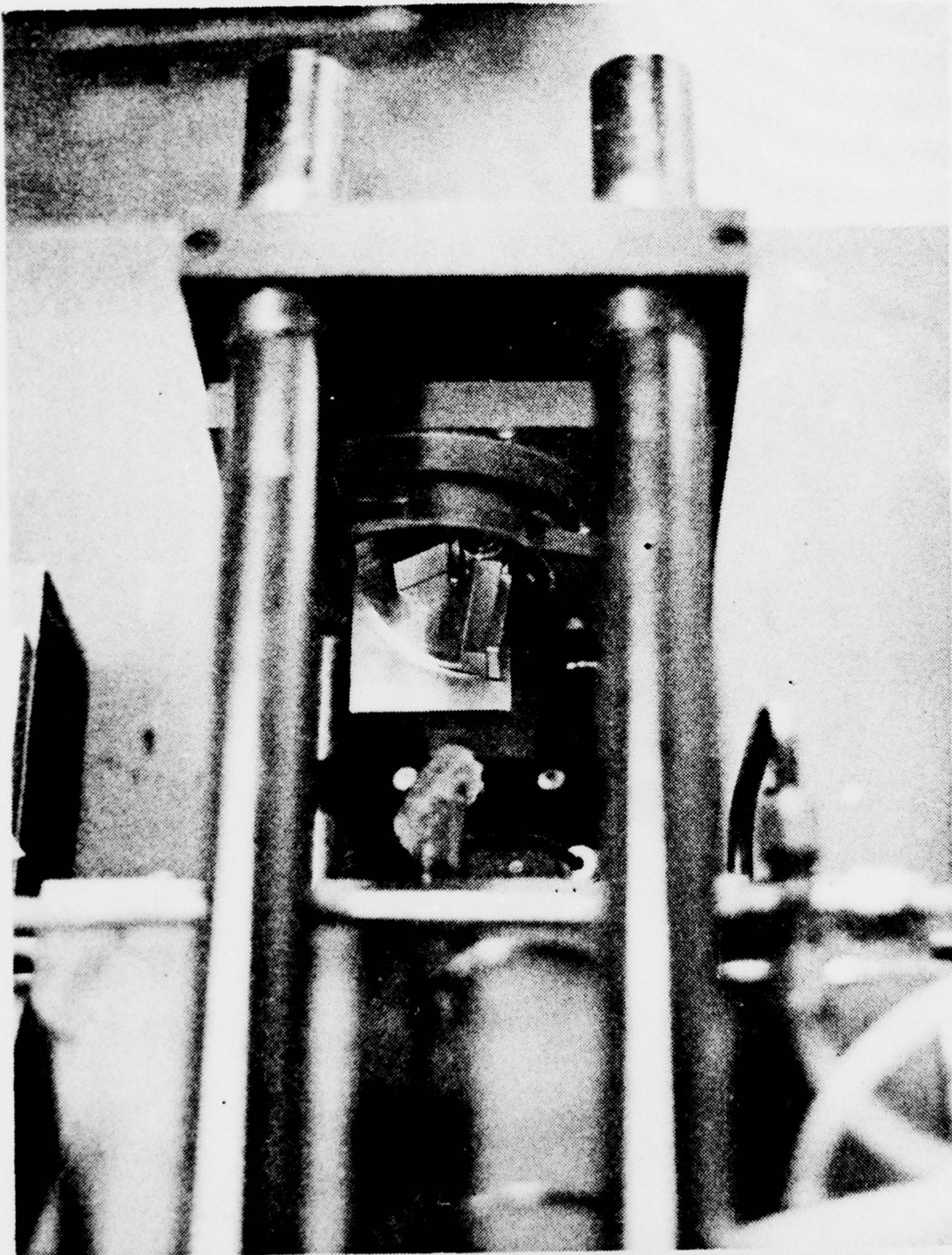


Figure 8 - TUNABLE SINGLE-LINE INSTALLATION

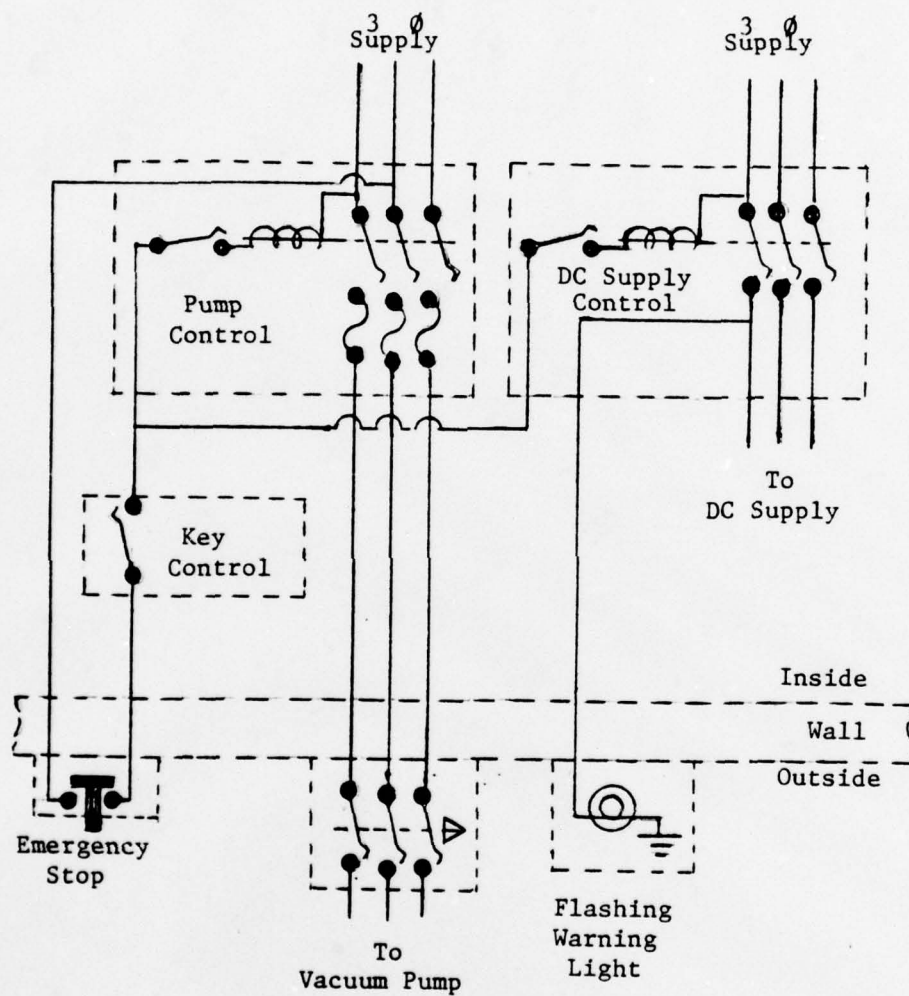


Figure 9 - ELECTRICAL SUPPLY SCHEMATIC





Figure 10 - LASER ROOM-EXTERNAL VIEW



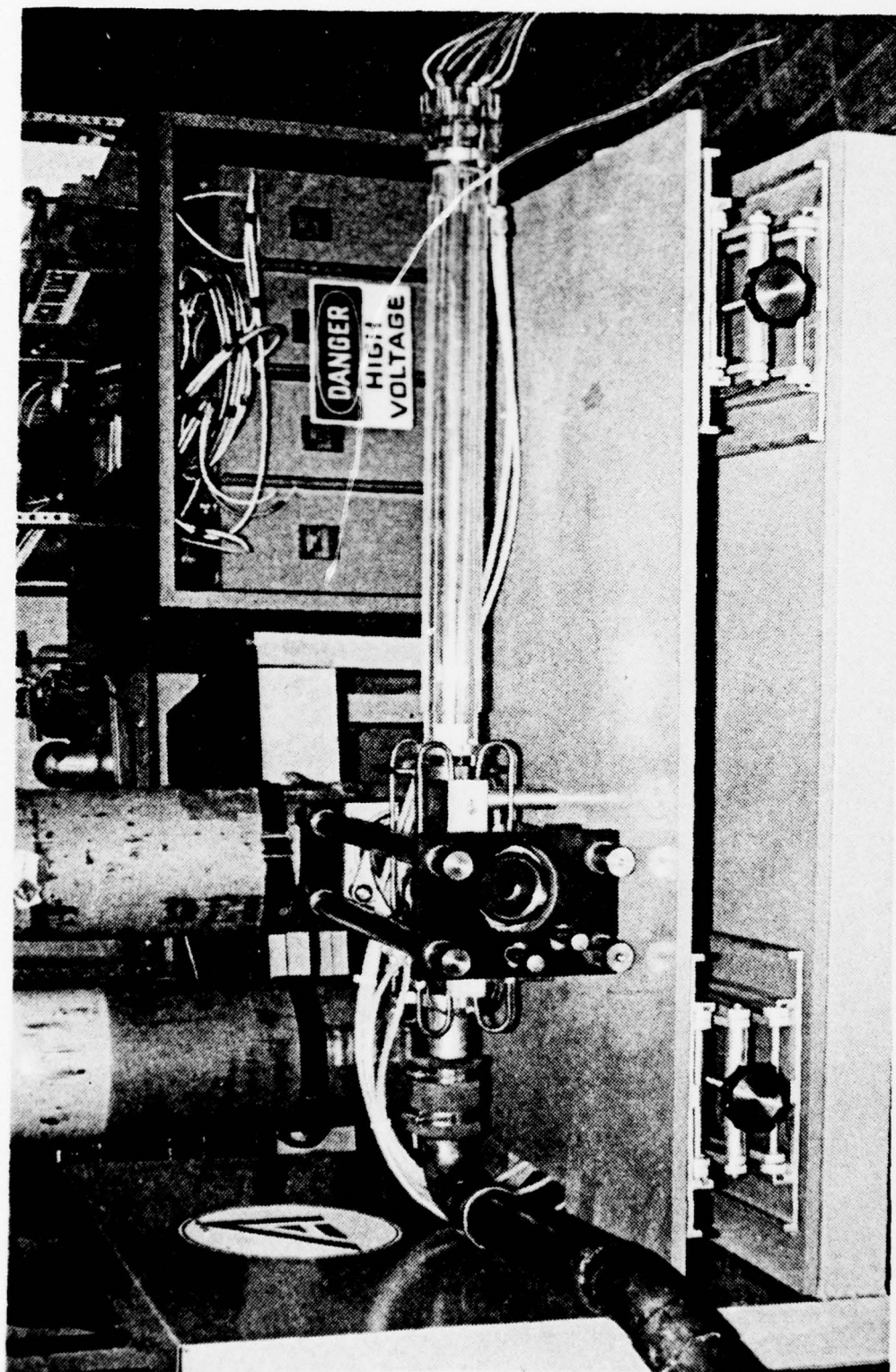


Figure 11 - LASER BENCH-TOP VIEW

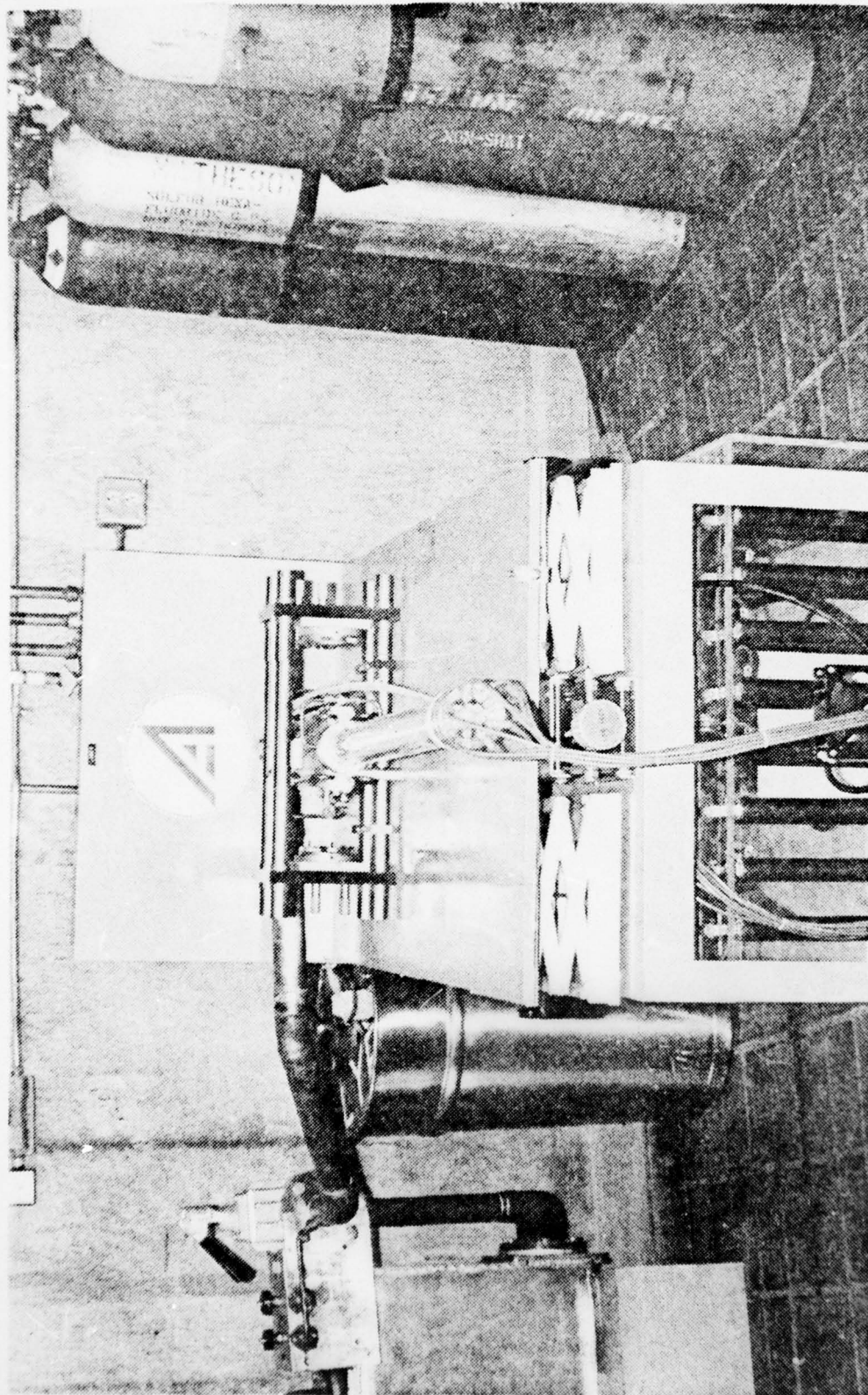


Figure 12 - LASER BENCH-FRONT VIEW

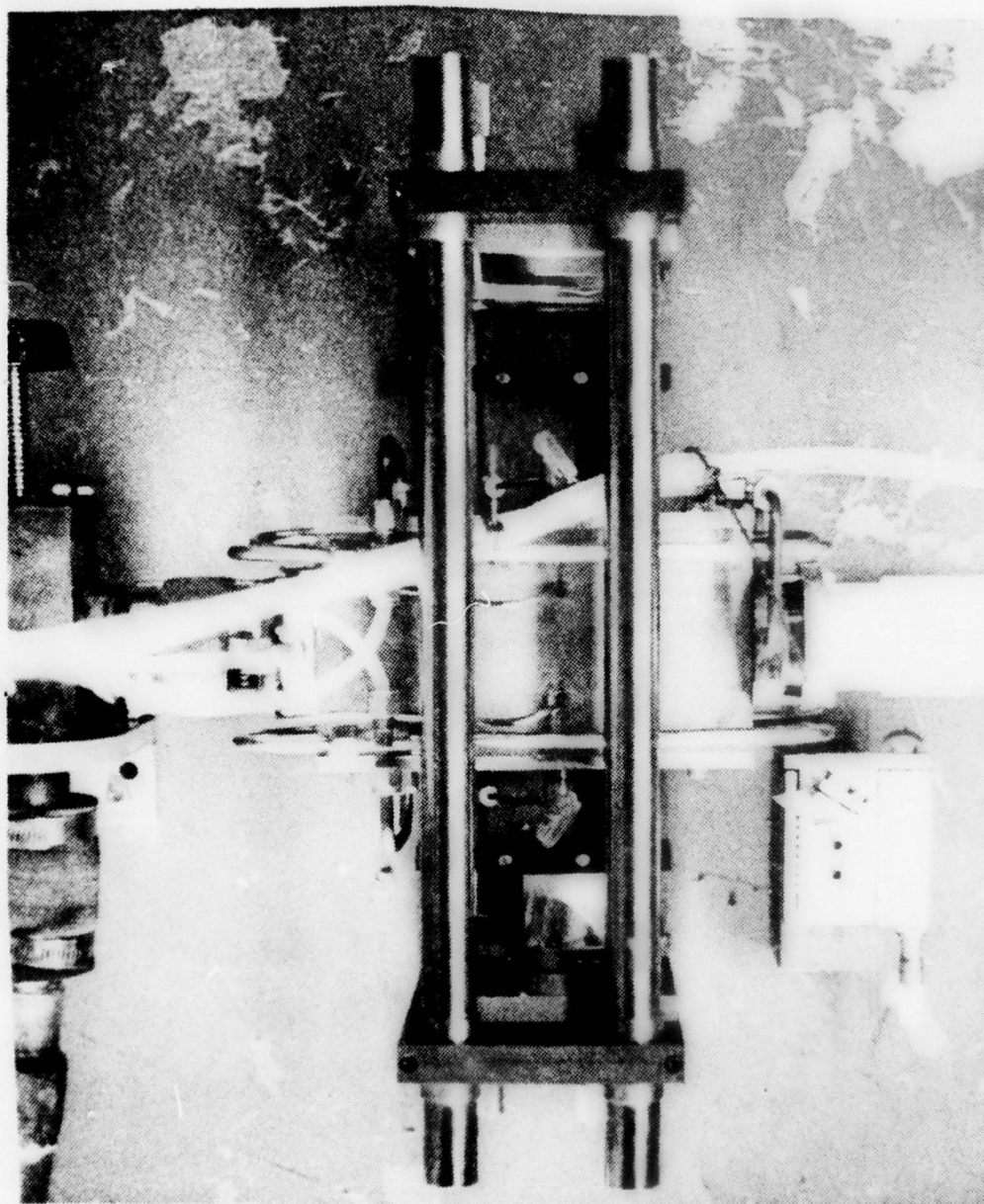


Figure 13 - LASER BENCH--SINGLE-LINE INSTALLATION



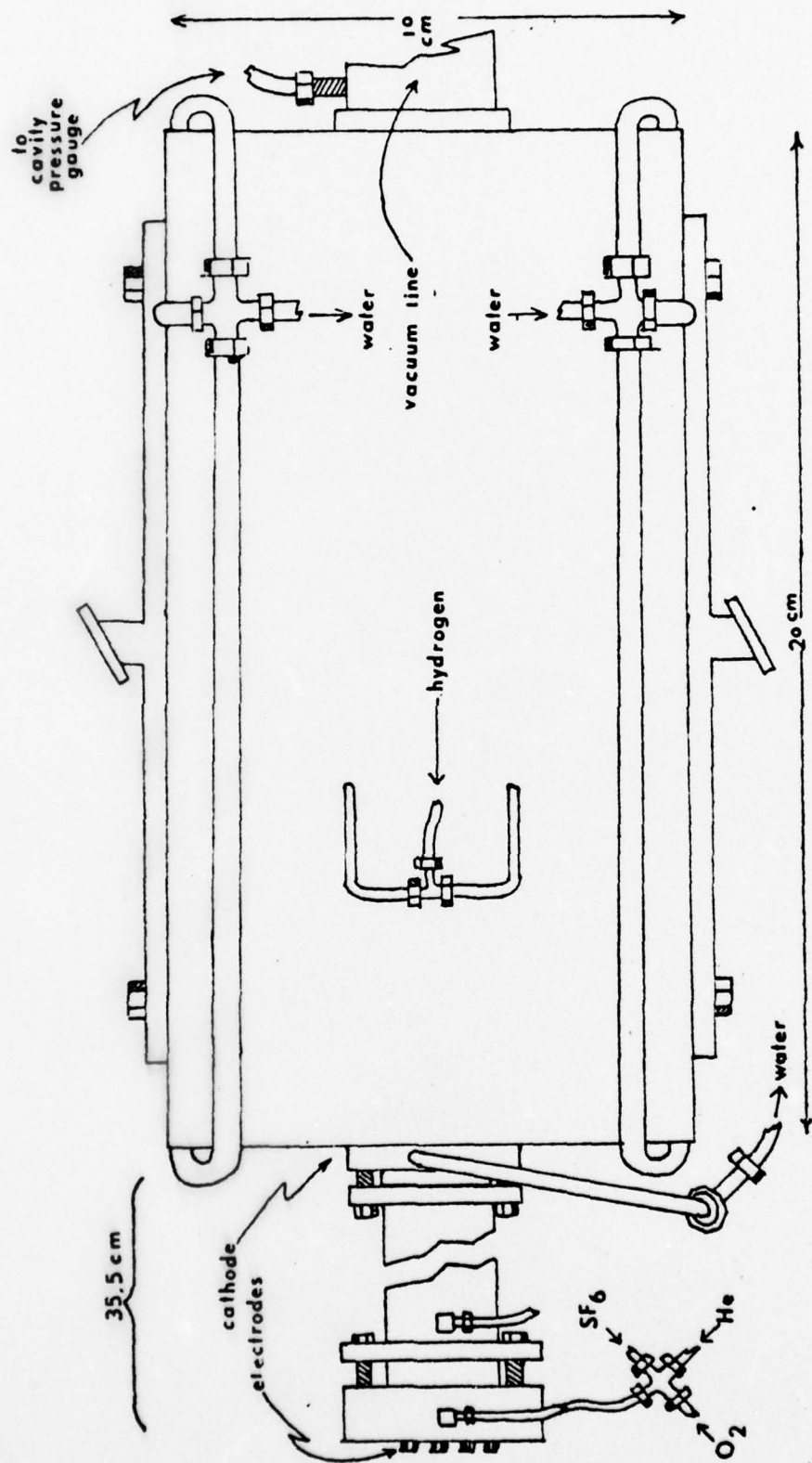
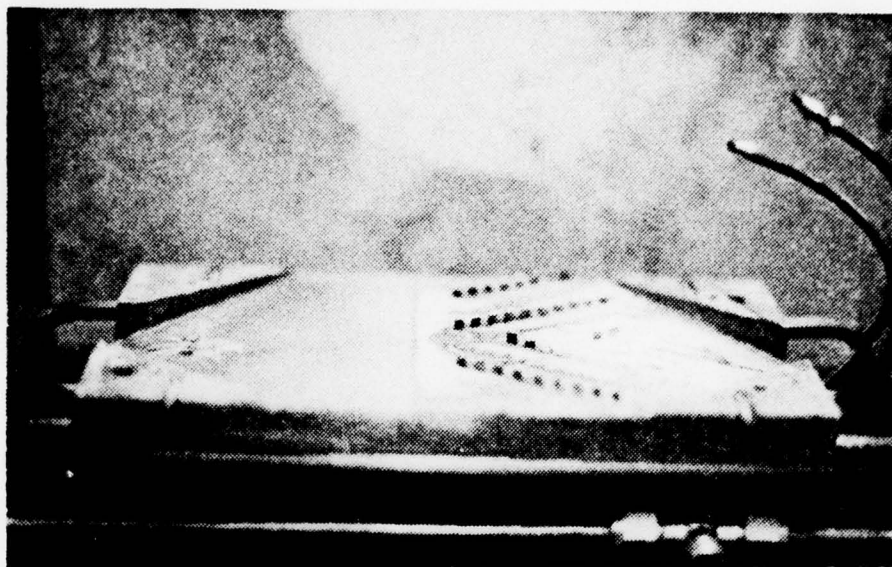
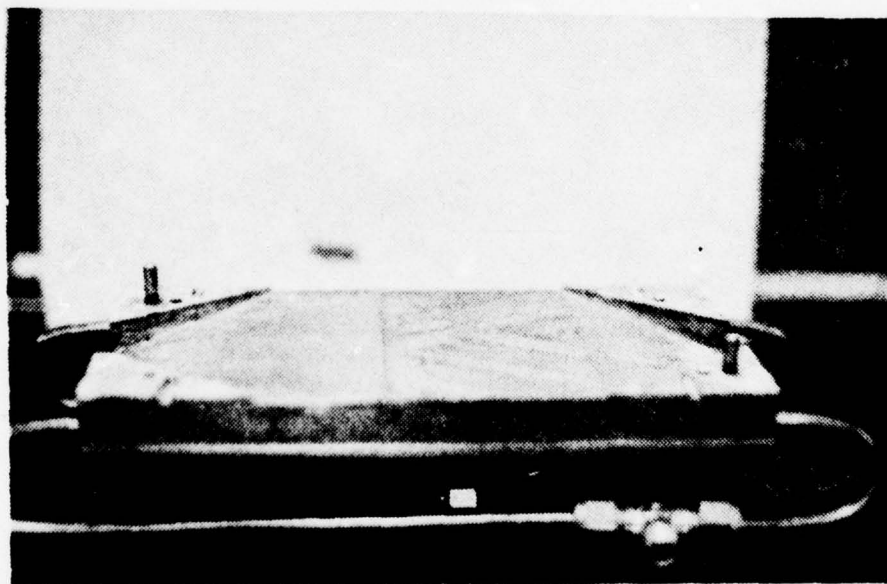


Figure 14 - THE MIXING CHAMBER DIAGRAM





A. Before Milling



B. After Milling

Figure 15 - THE MIXING CHAMBER OPENED .

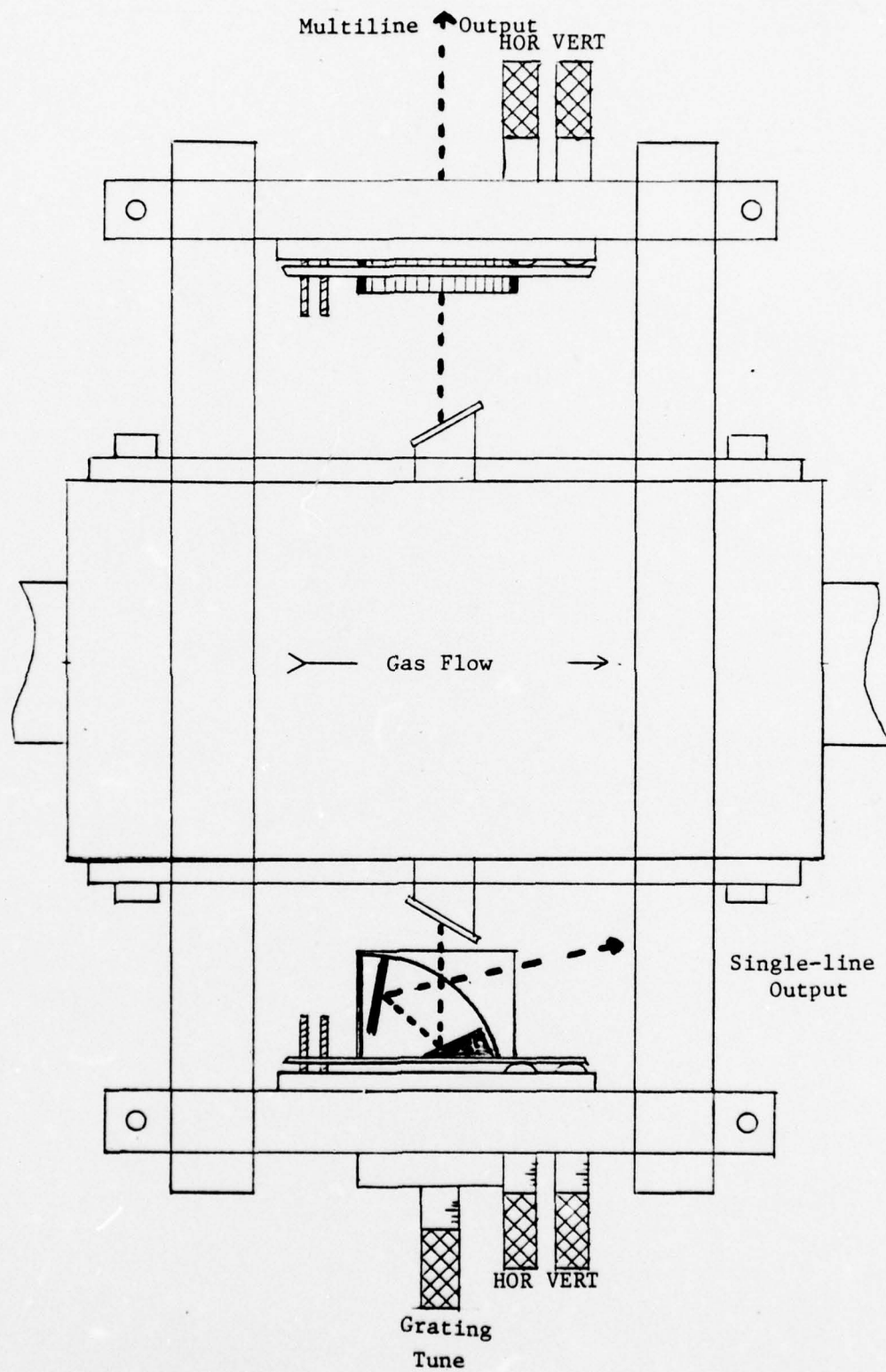


Figure 16 - THE OPTICAL RESONATOR

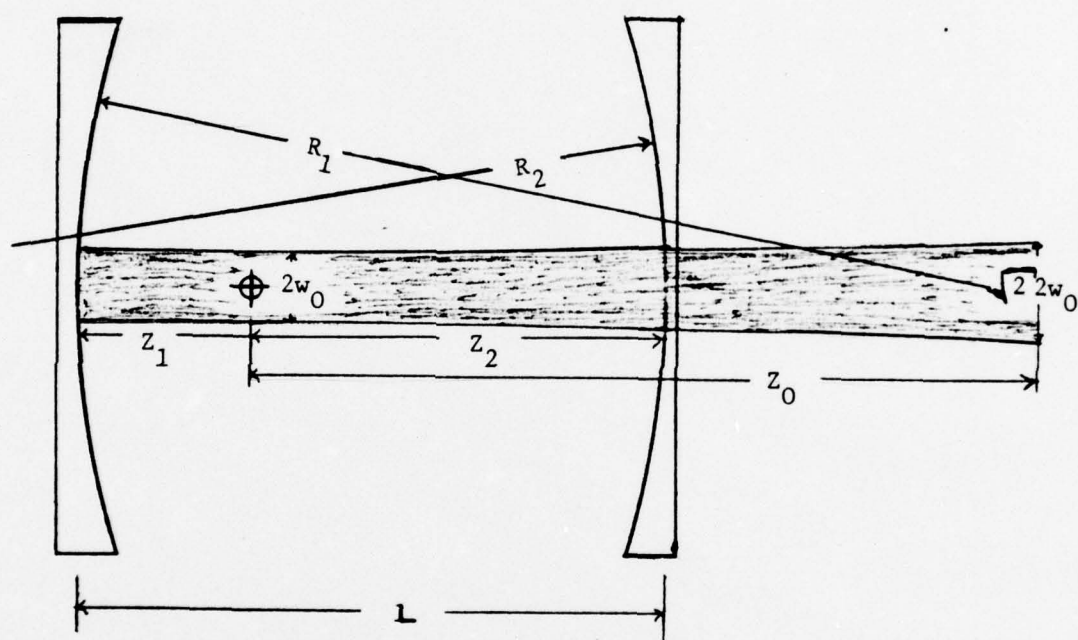


Figure 17 - THE GEOMETRY OF THE OPTICAL RESONATOR

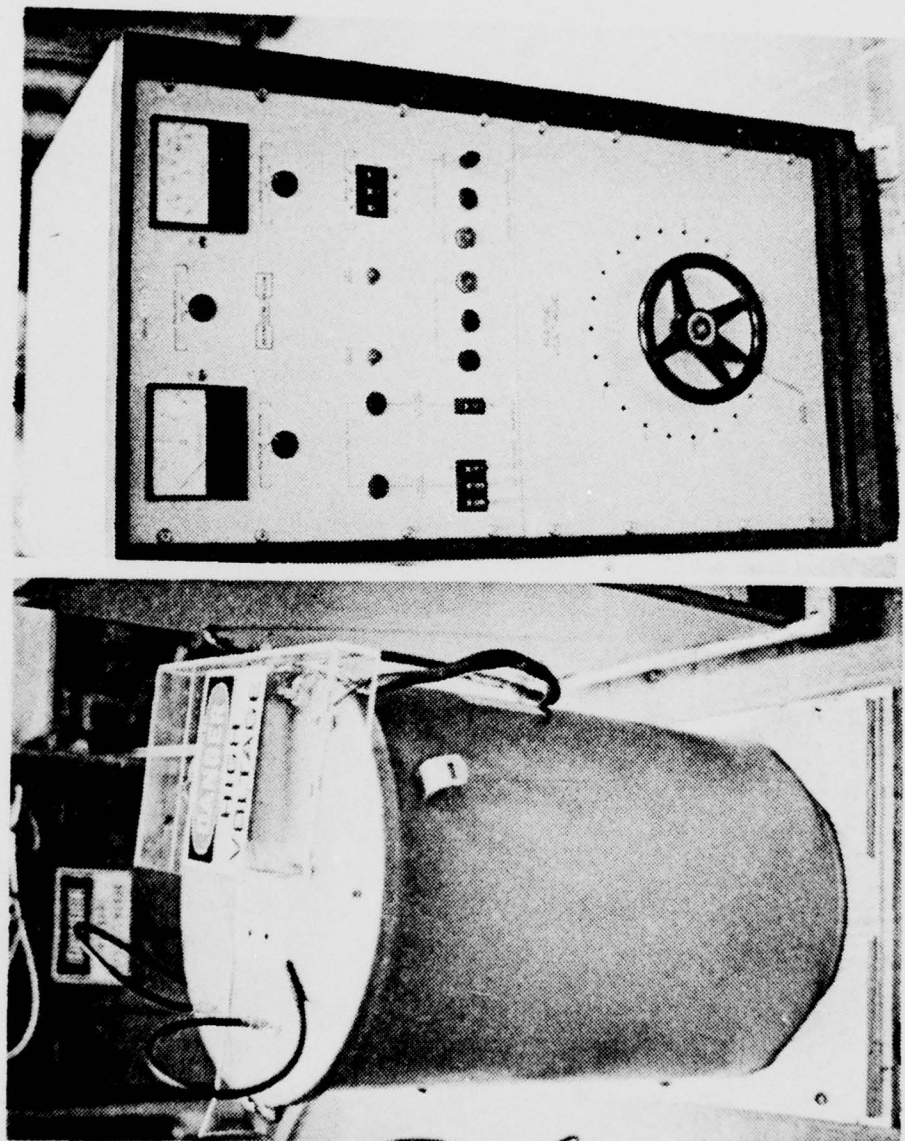


Figure 18 - THE DC POWER SUPPLY



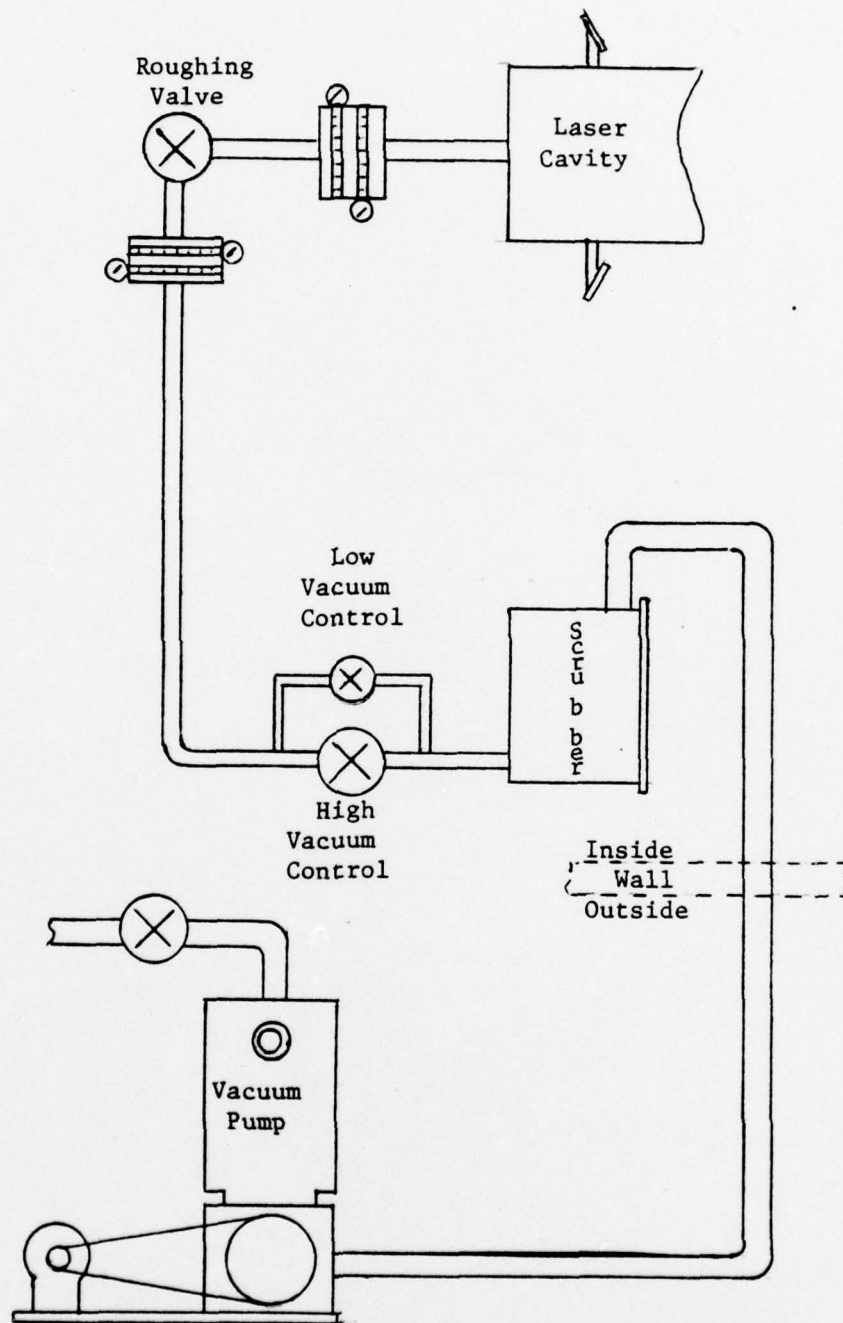


Figure 19 - VACUUM SYSTEM SCHEMATIC

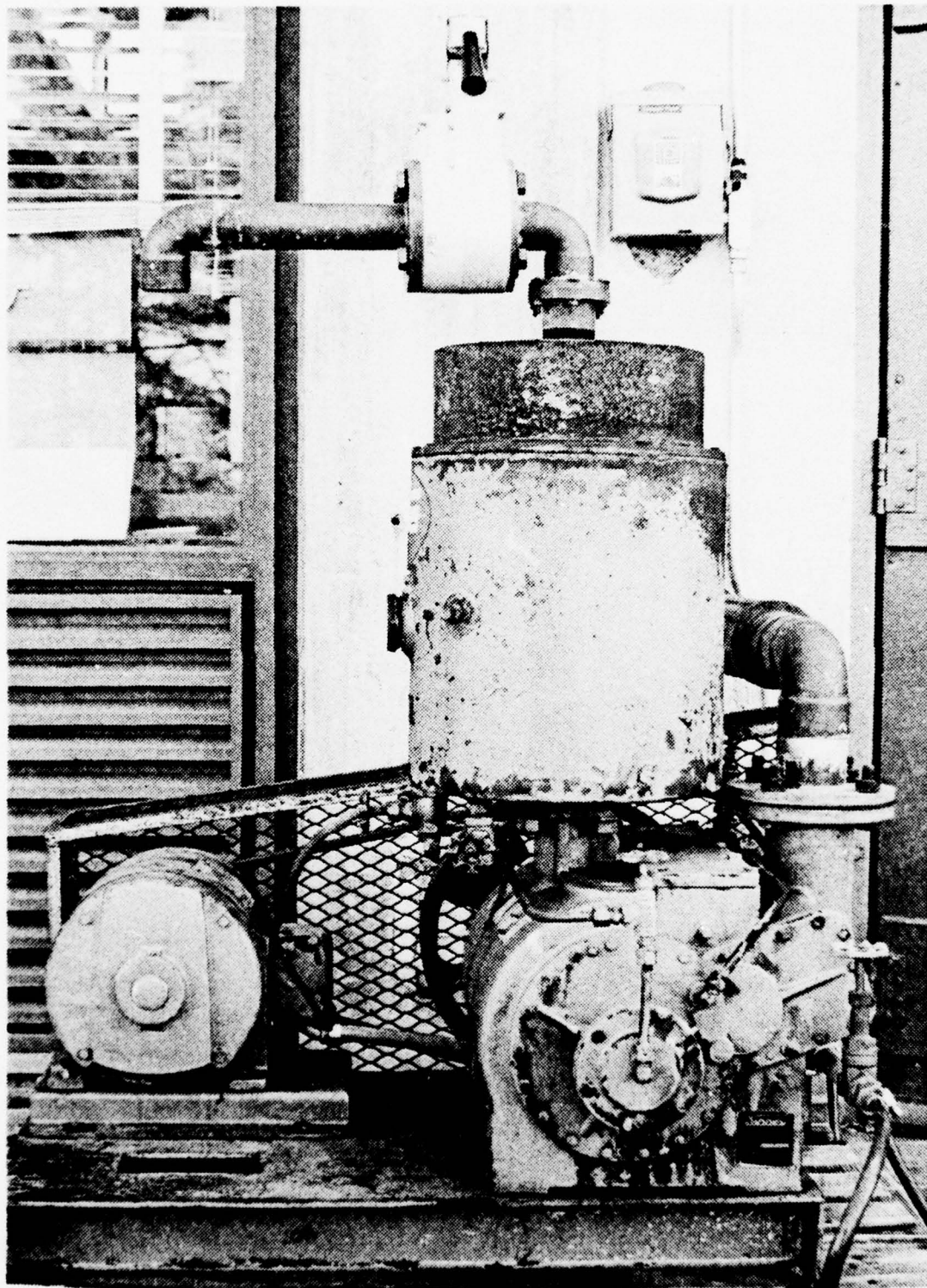


Figure 20 - VACUUM PUMP

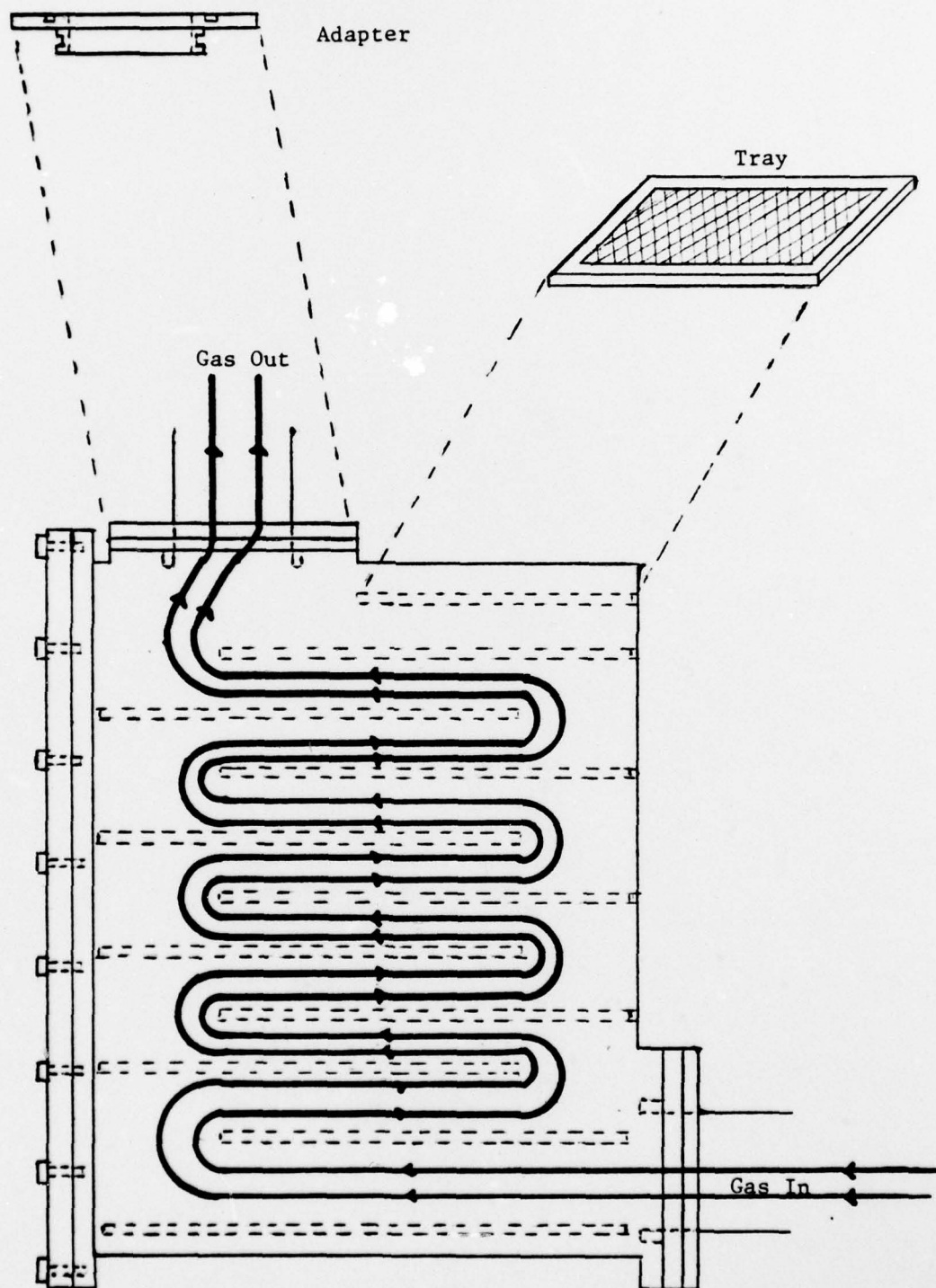


Figure 21 - SCRUBBER SYSTEM DIAGRAM



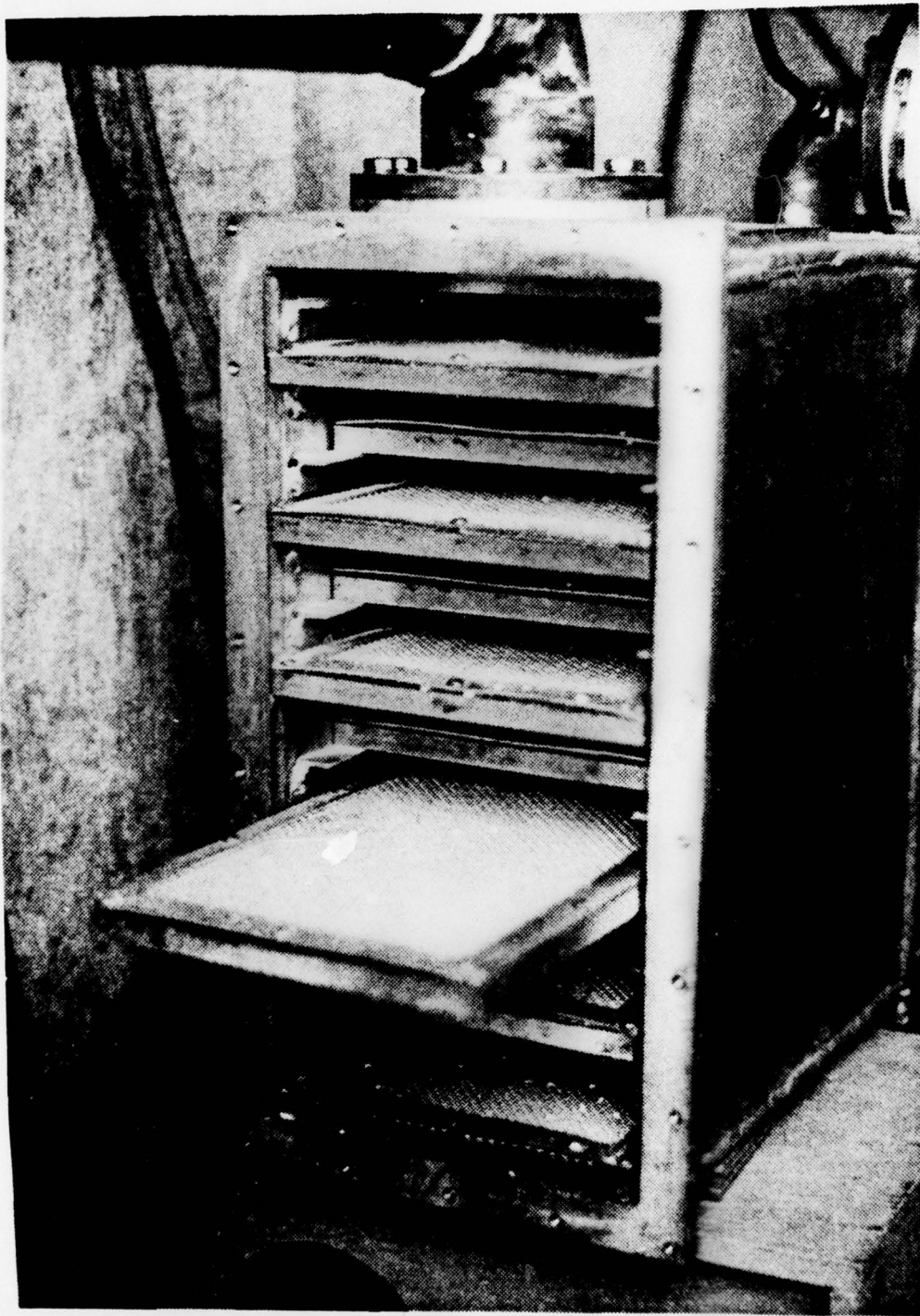


Figure 22 - SCRUBBER SYSTEM



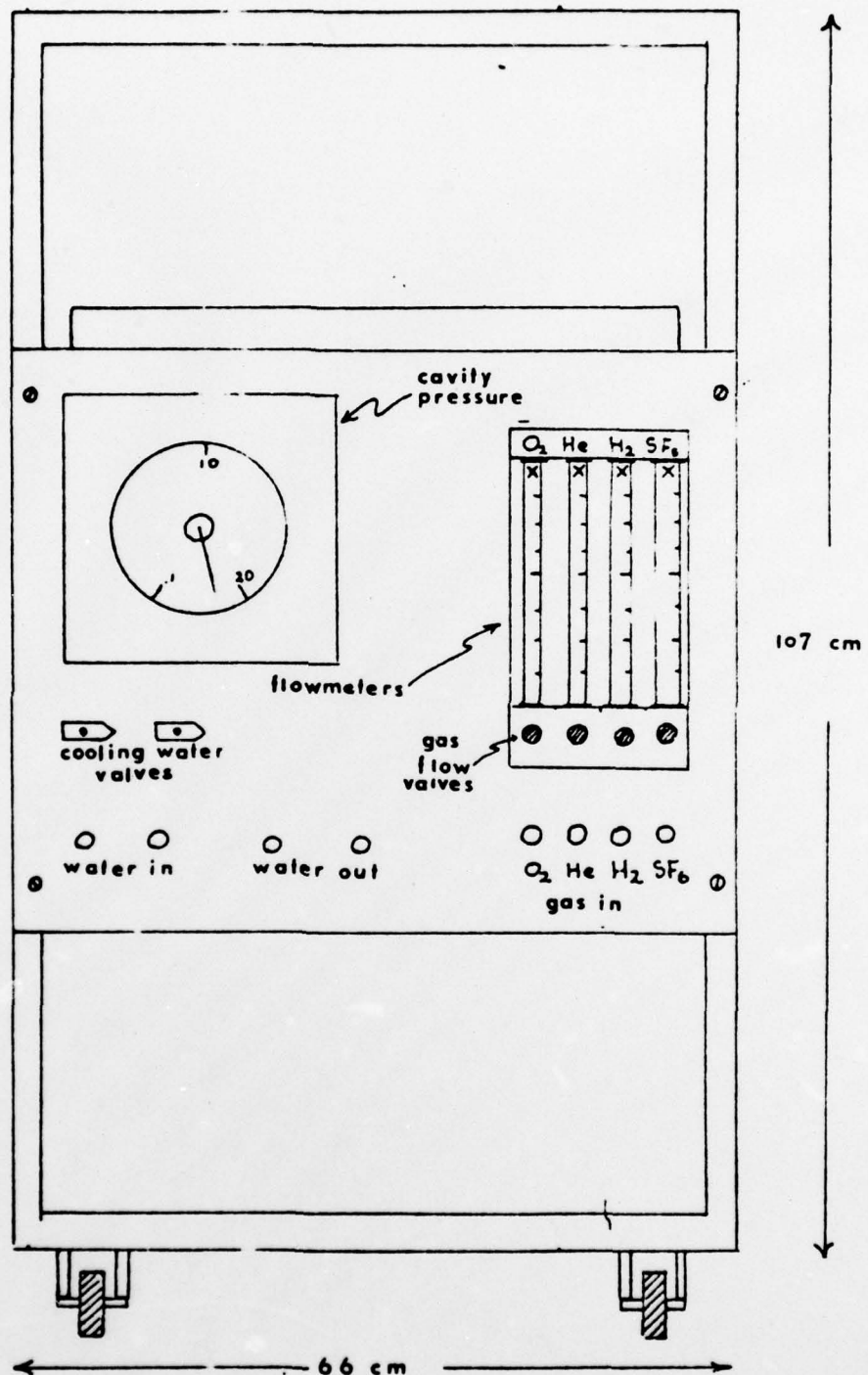


Figure 23 - LASER CONTROL PANEL DIAGRAM

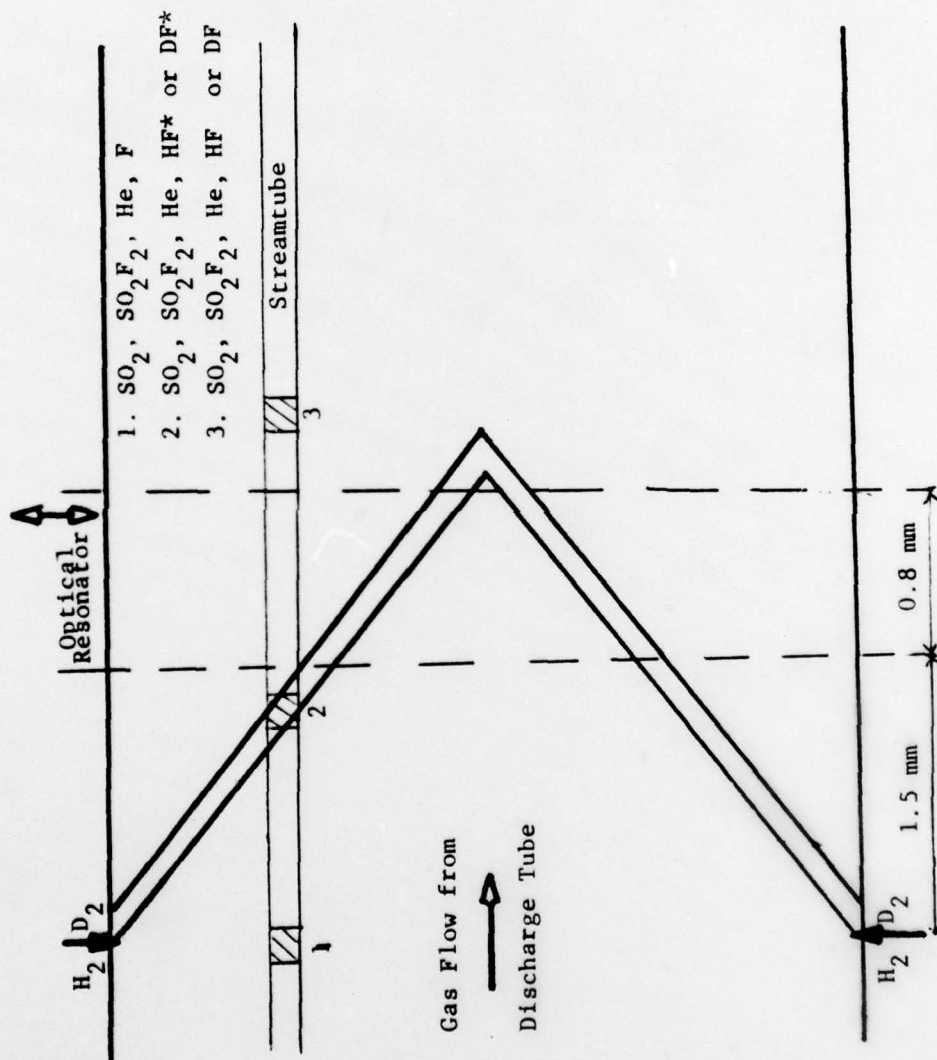


Figure 24 - HF/DF FLAME

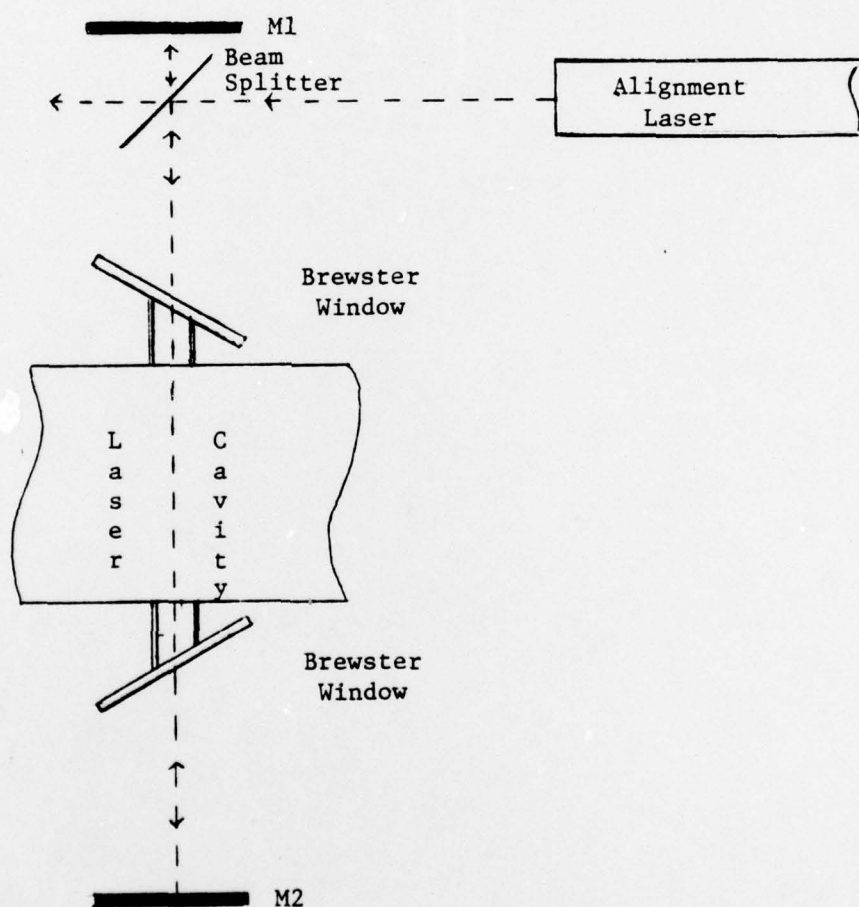


Figure 25 - LASER ALIGNMENT DIAGRAM

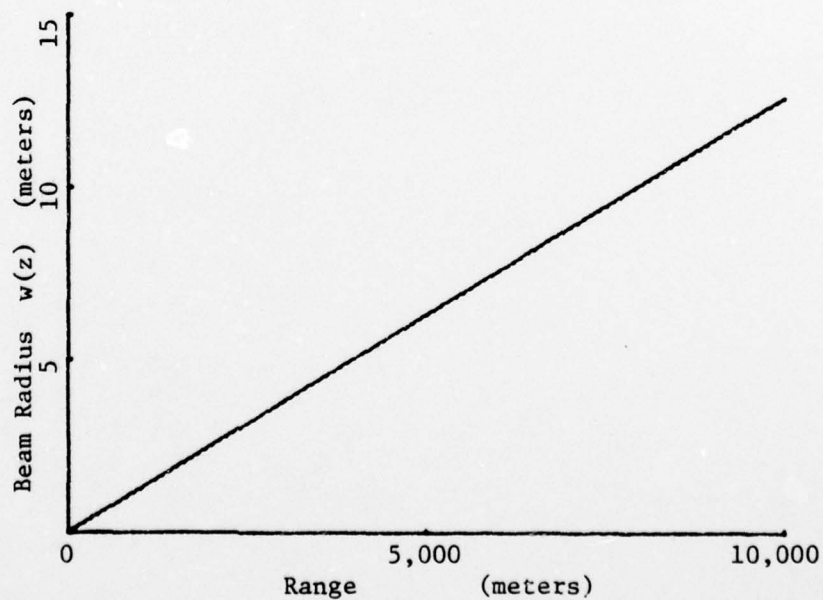
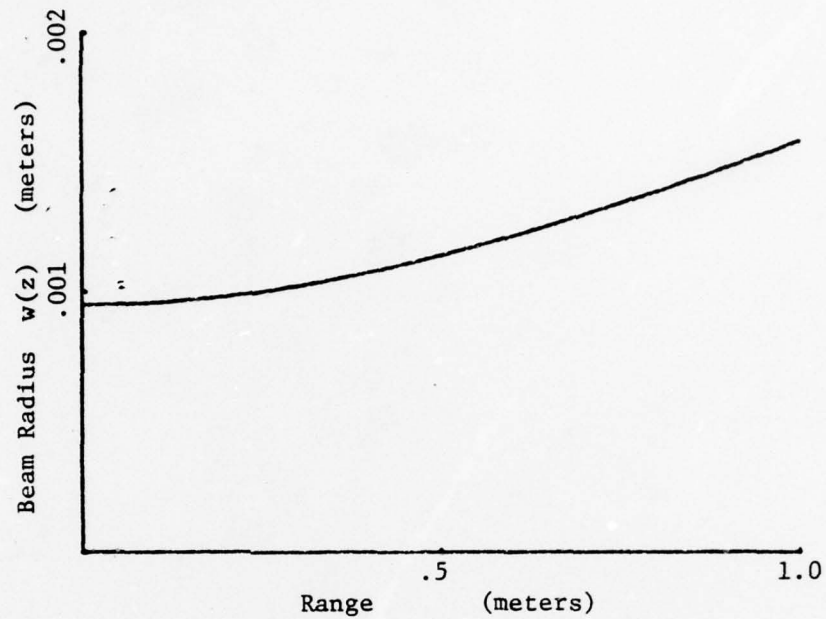
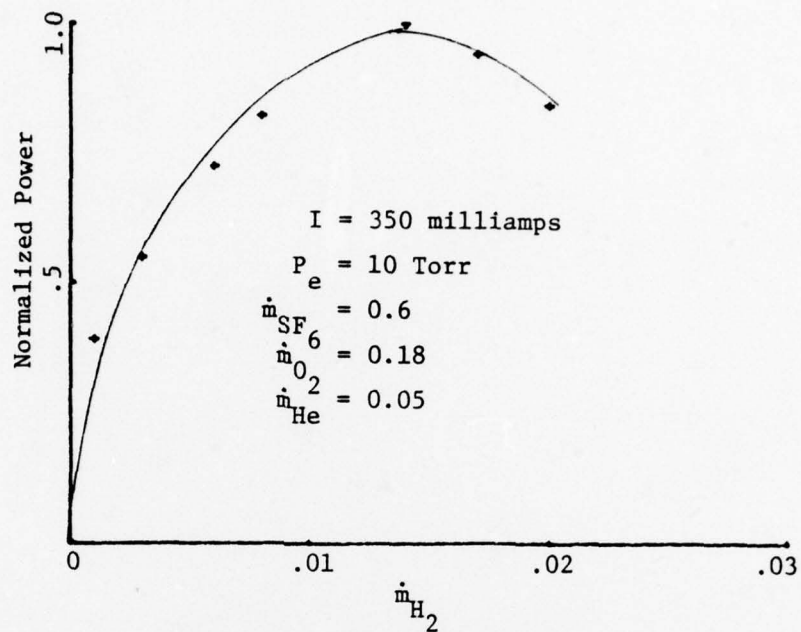
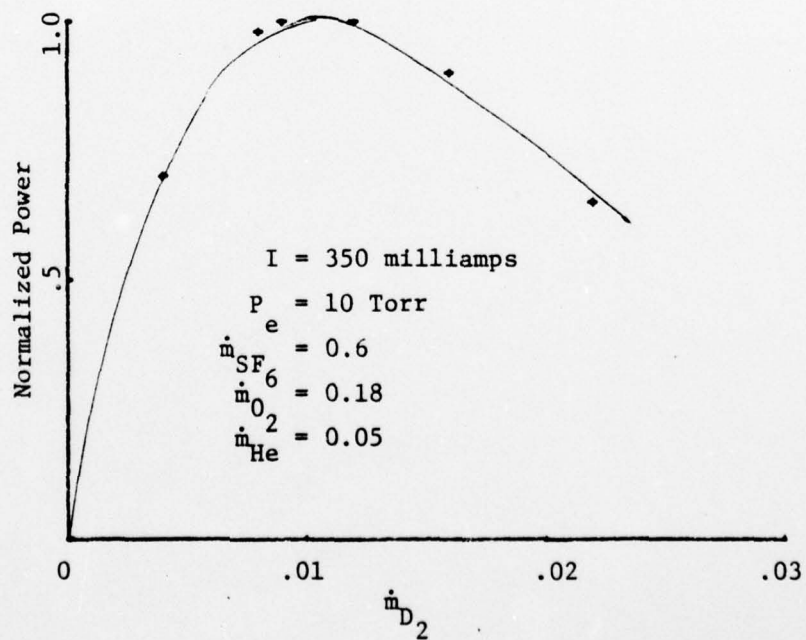


Figure 26 ~ BEAM RADIUS--DF SINGLE-LINE OPERATION





\* All flow rates gram/sec



\*All flow rates grams/sec

Figure 27 - OUTPUT POWER- $H_2$  OR  $D_2$  FLOW RATE VARIATIONS

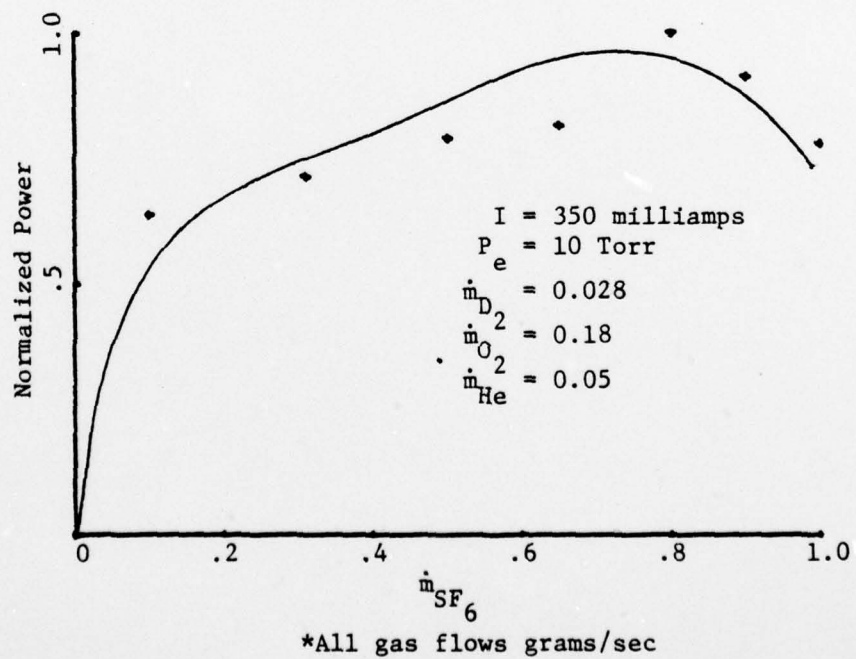
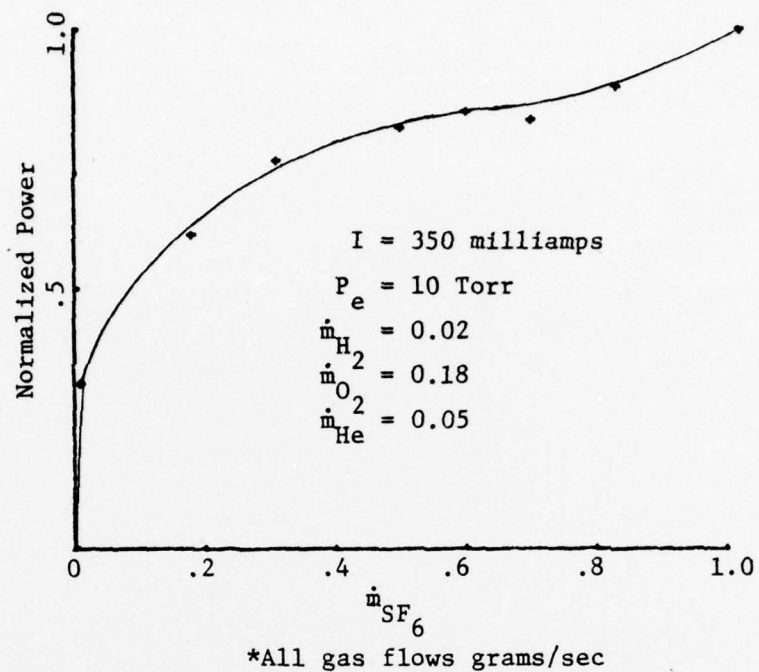
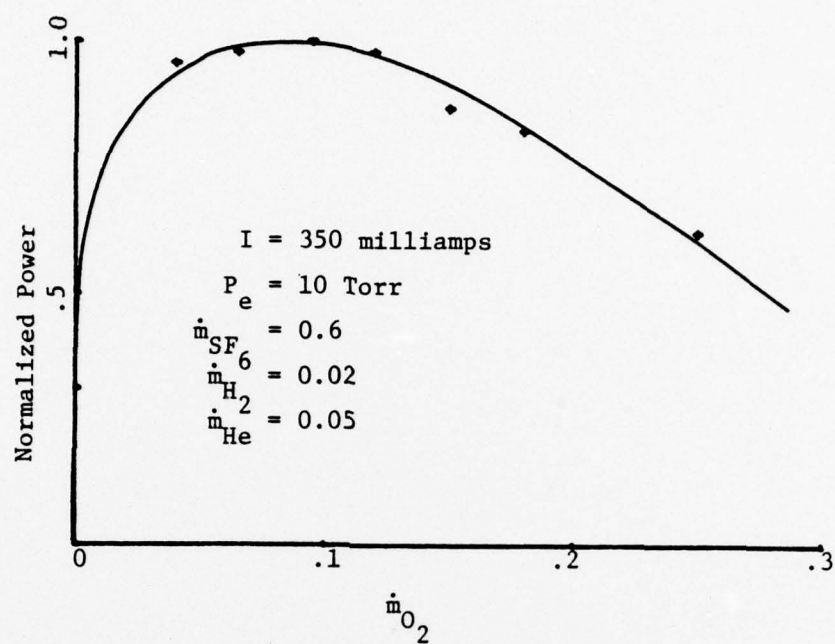
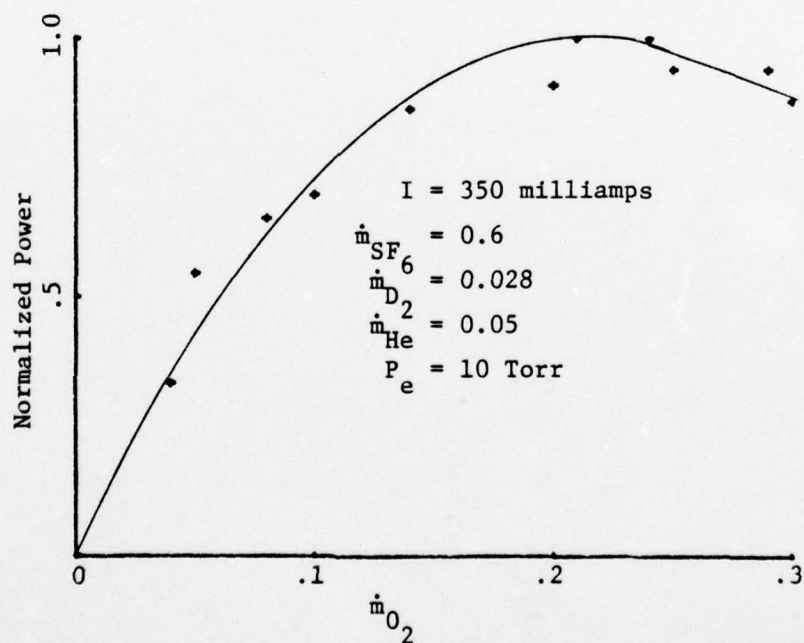


Figure 28 - OUTPUT POWER- $SF_6$  FLOW RATE VARIATIONS



\*All flow rates grams/sec



\*All flow rates grams/sec

Figure 29 - OUTPUT POWER- $O_2$  FLOW RATE VARIATIONS

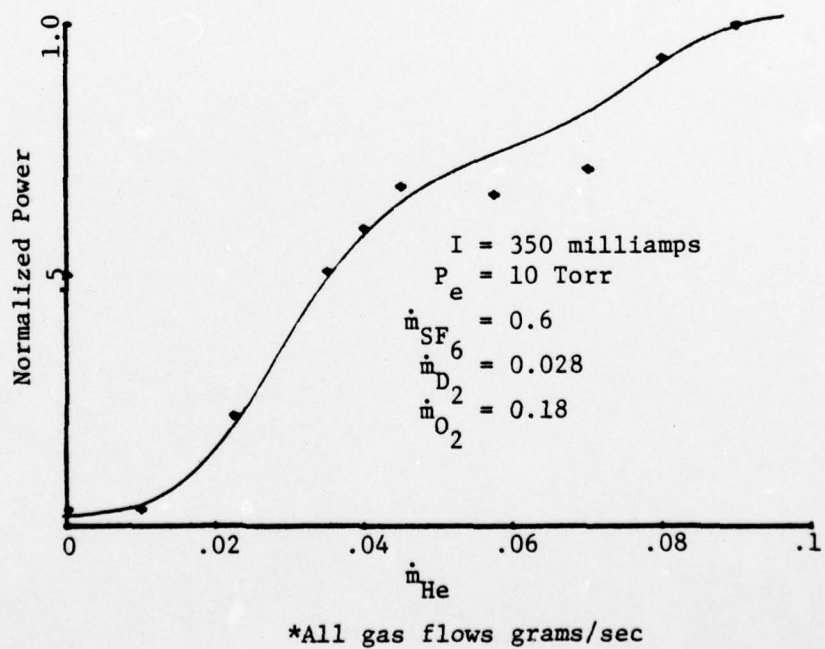
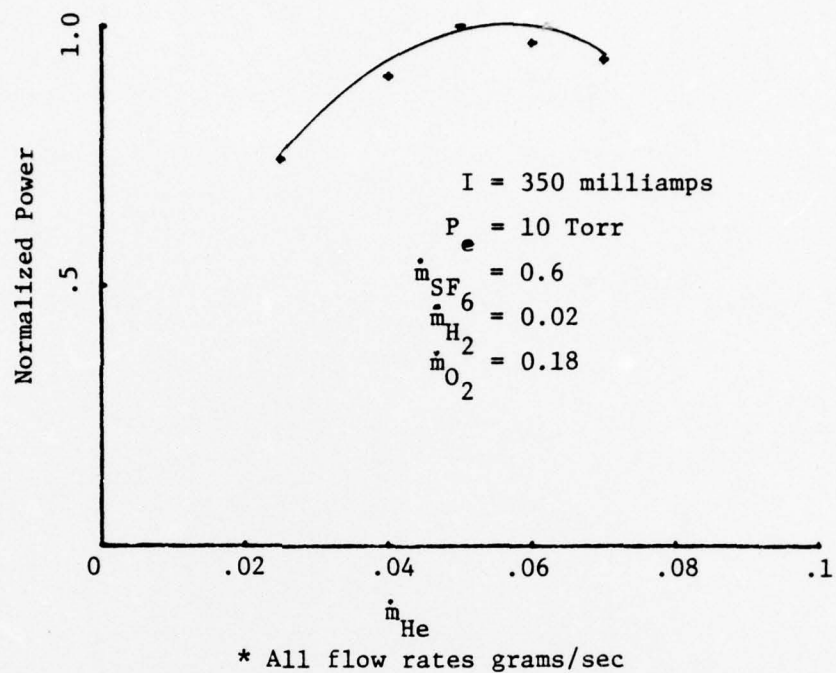


Figure 30 - OUTPUT POWER-He FLOW RATE VARIATIONS



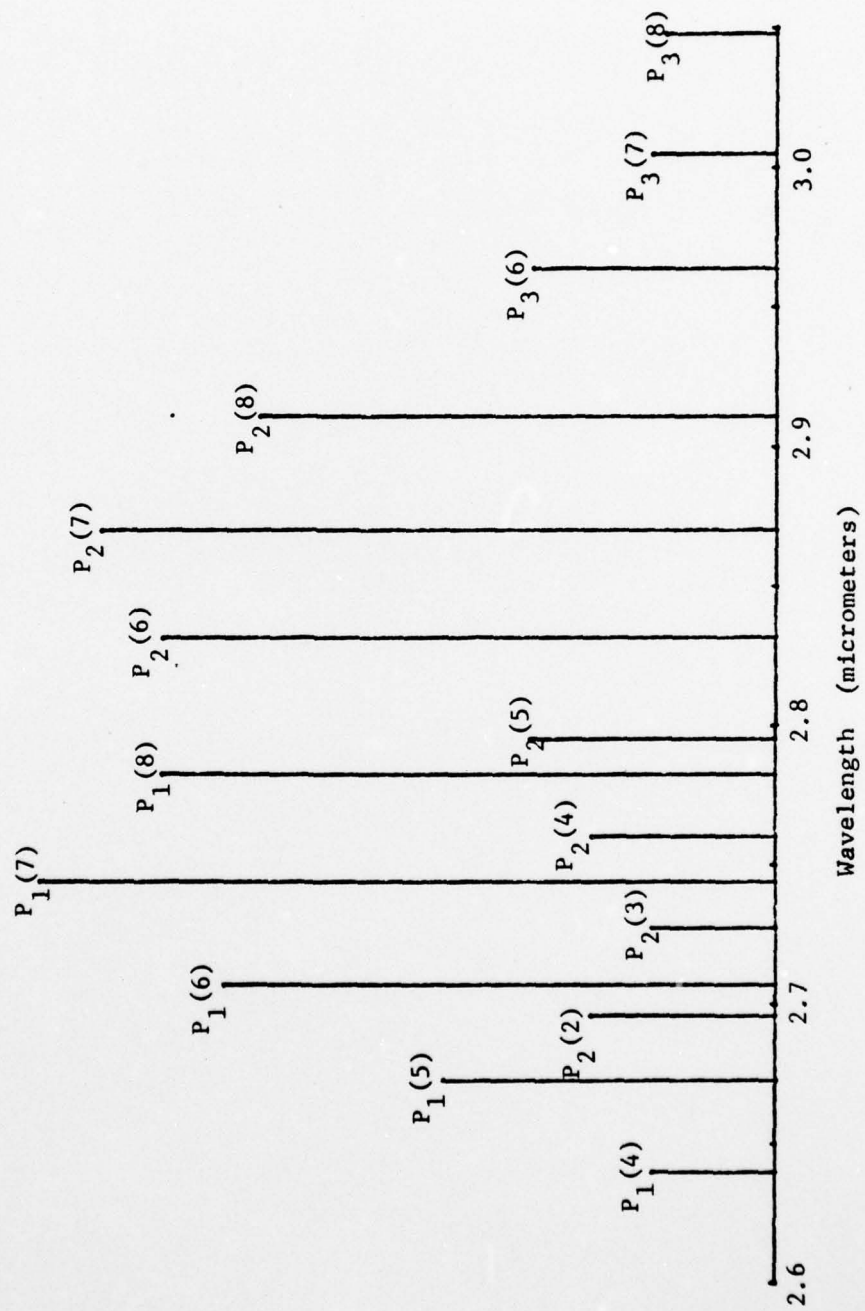


Figure 31 - HF WAVELENGTHS

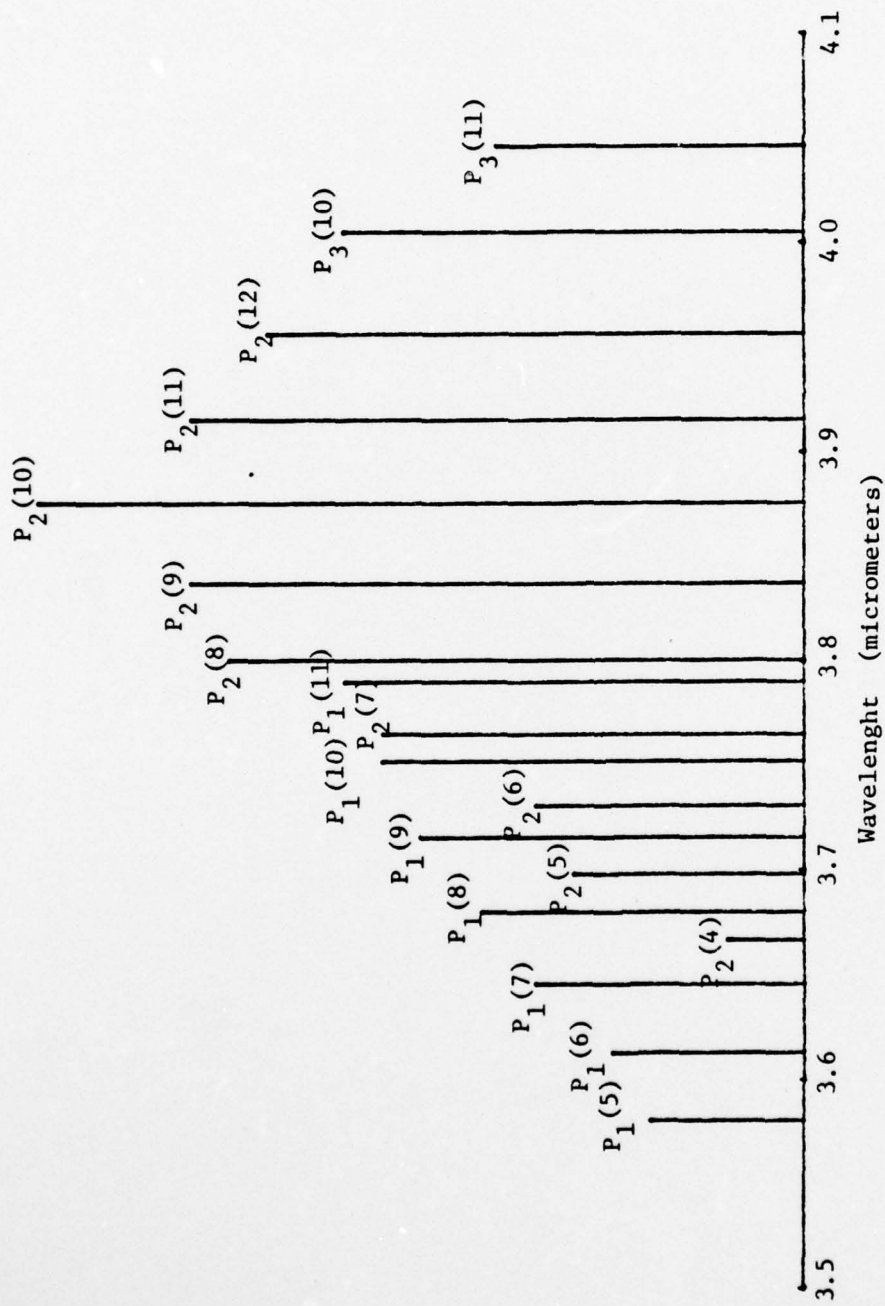


Figure 32 - DF WAVELENGTHS

#### LIST OF REFERENCES

1. Wolfe, W.I., Handbook of Military Infrared Technology, p. 175-281, Office of Naval Research, Washington, 1965.
2. Pressley, R.J., Handbook of Lasers with Selected Data on Optical Technology, p. 51-56, The Chemical Rubber Co., Cleveland, 1971.
3. Gross, R.W.F. and Spencer, D.J., Continuous Wave Hydrogen Halide Lasers, unpublished paper, Aerospace Corporation, El Segundo, Ca., 1974.
4. Tolles, W.M., Lecture and class notes presented as part of PH 3951, Quantum Mechanics, at the Naval Postgraduate School, 1976.
5. Cook, J.B., Construction of a Deuterium Fluoride Laser, M.S. Thesis, Naval Postgraduate School, Monterey, Ca., December 1975.
6. Mirels, H. and Spencer, D.J., "Power and Efficiency of a Continuous HF Chemical Laser", IEEE Journal of Quantum Electronics, v. QE-7, p. 501-507, November, 1971.
7. Ryss, I.G., The Chemistry of Fluorine and its Inorganic Compounds, Part 1, State Publishing House for Technical, Scientific, and Chemical Literature, Moscow, 1956.
8. Banas, C.M. and Hitchen, J.J., "cw HF Electric-Discharge Mixing Laser", Applied Physics Letters, v. 17, p. 386-388, November 1970.

9. Spencer,D.J., Mirels,H., and Durran,D.A., "Performance of cw HF Chemical Laser with N<sub>2</sub> or He Diluent", Journal of Applied Physics, v. 43, p. 1151-1157, March 1972.
10. U.S. Army Missile Command Final Technical Report, Investigation of Chemical Lasers, by J.R. Airey and S.S. Fried, p.3-4, November 1970.
11. Yariv, A., Introduction to Optical Electronics, 2d ed., p. 58-88, Holt, Rhinehart and Winston, 1976.
12. Pilar, F.L., Elementary Quantum Chemistry, p. 259-266, McGraw-Hill, 1968.
13. Spencer,D.J., Beggs,J.A.,and Mirels,H., "Small-scale cw HF(DF) Chemical Laser", Journal of Applied Physics, v. 48, p. 1206-1211, March, 1977.



# INITIAL DISTRIBUTION LIST

	No. Copies
1. Defense Documentation Center Cameron Station Alexandria, Virginia 22314	2
2. Chairman, Dept. of Physics and Chemistry Code 61 Naval Postgraduate School Monterey, California 93940	2
3. Library Code 0212 Naval Postgraduate School Monterey, California 93940	2
4. Dr. A. W. Cooper Code 61cr Naval Postgraduate School Monterey, California 93940	4
5. Mr. Kenneth Graham, Chemist Code 61Kg, Naval Postgraduate School Monterey, Ca., 93940	1
6. LT William T. Funk, USN Route # 2 Lena, Wisconsin 54139	1
7. LT Richard F. Sontheimer, USN Admin Unit NAU/NROTC Unit MIT Cambridge, Ma. 02139	1